Pergamon

Geochimica et Cosmochimica Acta, Vol. 68, No. 10, pp. 2295–2311, 2004

0016-7037/04 $30.00 + .00

doi:10.1016/j.gca.2003.11.029

Subsurface processes at the Lucky Strike hydrothermal field, Mid-Atlantic Ridge: Evidence from sulfur, selenium, and iron isotopes

OLIVIER ROUXEL,[1,*] YVES FOUQUET,[2] and JOHN N. LUDDEN[1]

[1]CRPG-CNRS, 15 rue Notre Dame des Pauvres, 54501 Vandoeuvre les Nancy, France
[2]IFREMER DRO/GM, BP 70, 29280 Plouzané, France

(*Received December* 9, 2002; *accepted in revised form November* 18, 2003)

Abstract—At Lucky Strike near the Azores Triple Junction, the seafloor setting of the hydrothermal field in a caldera system with abundant low-permeability layers of cemented breccia, provides a unique opportunity to study the influence of subsurface geological conditions on the hydrothermal fluid evolution. Coupled analyses of S isotopes performed in conjunction with Se and Fe isotopes have been applied for the first time to the study of seafloor hydrothermal systems. These data provide a tool for resolving the different abiotic and potential biotic near-surface hydrothermal reactions. The $\delta^{34}S$ (between 1.5‰ and 4.6‰) and Se values (between 213 and 1640 ppm) of chalcopyrite suggest a high temperature end-member hydrothermal fluid with a dual source of sulfur: sulfur that was leached from basaltic rocks, and sulfur derived from the reduction of seawater sulfate. In contrast, pyrite and marcasite generally have lower $\delta^{34}S$ within the range of magmatic values (0 ± 1‰) and are characterized by low concentrations of Se (<50 ppm). For $^{82}Se/^{76}Se$ ratios, the $\delta^{82}Se$ values range from basaltic values of near −1.5‰ to −7‰. The large range and highly negative values of hydrothermal deposits observed cannot be explained by simple mixing between Se leached from igneous rock and Se derived from seawater. We interpret the Se isotope signature to be a result of leaching and mixing of a fractionated Se source located beneath hydrothermal chimneys in the hydrothermal fluid. At Lucky Strike we consider two sources for S and Se: (1) the "end-member" hydrothermal fluid with basaltic Se isotopic values (−1.5‰) and typical S isotope hydrothermal values of 1.5‰; (2) a fractionated source hosted in subsurface environment with negative $\delta^{34}S$ values, probably from bacterial reduction of seawater sulfate and negative $\delta^{82}Se$ values possibly derived from inorganic reduction of Se oxyanions. Fluid trapped in the subsurface environment is conductively cooled and has restricted mixing and provide favorable conditions for subsurface microbial activity which is potentially recorded by S isotopes. Fe isotope systematic reveals that Se-rich high temperature samples have $\delta^{57}Fe$ values close to basaltic values (~0‰) whereas Se-depleted samples precipitated at medium to low temperature are systematically lighter ($\delta^{57}Fe$ values between −1 to −3‰). An important implication of our finding is that light Fe isotope composition down to −3.2‰ may be explained entirely by abiotic fractionation, in which a reservoir effect during sulfide precipitation was able to produce highly fractionated compositions.

1. INTRODUCTION

Recent findings have extended the biosphere to include the microbial life hosted in deep subsurface regions of the Earth's crust. This deep biosphere occurs within continental crust (Fredrickson and Onstott, 1996), terrestrial basalts (Stevens and McKinley, 1995), deep-sea sediments (Parkes et al., 1994), deep oil reservoirs (Stetter et al., 1993) and at seafloor hydrothermal vents at mid ocean ridges (Delaney et al., 1998) and the associated volcanic rocks (Fisk et al., 1998). The subseafloor at midocean ridges is an excellent microbial habitat, because there is abundant space, fluid flow, and geochemical energy in the porous, hydrothermally influenced oceanic crust. Subsurface environments, where mixing of hot (~350°C) hydrothermal fluids and cold seawater occurs, are predicted to be energy-rich and may harbor large and diverse microbial communities (Deming and Baross, 1993; Wirsen et al., 1993; Jannasch, 1995; McCollom and Shock, 1997; Delaney et al., 1998; Summit and Baross, 2001). Microbes living in subsurface mixing zones and within chimney walls (Takai et al., 2001) may affect the speciation and distribution of metals, (i.e., Fe and Mn), and metalloids such as S and potentially Se through redox reactions, such as the dissimilatory reduction of oxyanions or oxidation of reduced compounds (Wirsen et al., 1993; Jannasch, 1995; McCollom and Shock, 1997). They also influence these elements through the release of metabolic by-products into the environment, and, directly or indirectly, modify the rates and mechanisms of mineral dissolution and formation, by inducing mineral precipitation within or around cells.

Sulfur isotope studies provide valuable information for determining sulfur sources and precipitation mechanisms in submarine hydrothermal deposits. Different mechanisms have been proposed to explain variations in the $\delta^{34}S$ values of sulfides in seafloor hydrothermal systems (e.g., Shanks, 2001) and indicate that sulfur has two sources: (1) sulfur from the leaching of igneous rocks; (2) sulfur from the reduction of a small amount of admixed seawater-derived sulfate. Microbial sulfate reduction could be a possible alternative source of H_2S in seafloor hydrothermal system at temperatures below 100°C (L'Haridon et al., 1998; Jorgensen et al., 1992). However, the impact of sulfate-reducing microbes on sulfur isotope signature of hydrothermal sulfides has only been highlighted in sediment-covered hydrothermal systems (Peter and Shanks, 1992).

Over the past 5 yr scientists have successfully applied mul-

* Author to whom correspondence should be addressed, at Department of Earth Sciences, University of Cambridge, Downing Street, Cambridge CB2 3EQ, UK (orou02@esc.cam.ac.uk).

tiple-collector inductively coupled plasma mass spectrometry (MC-ICP-MS) to the precise measurement of stable isotopes of metals that may provide useful geochemical tracers in seafloor hydrothermal systems. Such elements include Cu, Fe and Zn (Maréchal et al., 1999; Belshaw et al., 2000; Zhu et al., 2000a) and metalloids such as Se (Rouxel et al., 2002).

The use of Fe isotopes to trace geochemical and biologic cycling of Fe has received a great interest in the past few years (Beard et al., 2003a, and references therein). Laboratory evidence of microbe-induced Fe isotope fractionation (Beard et al., 1999; Brantley et al., 2001) suggests that Fe isotope studies could be used to trace biologic activity in natural environments. In seafloor hydrothermal systems, bacterial iron reduction is a common process (Vargas et al., 1998; Slobodkin et al., 2001) and iron-oxidizing microorganisms play an important role in the formation of iron oxide deposits at seafloor (Juniper and Fouquet, 1988). Therefore, Fe isotope geochemistry may provide important insights into biologic processes at deep-sea vents. Se isotopes are known to fractionate during microbially-mediated reduction (Krouse and Thode, 1962; Herbel et al., 2000; Ellis et al., 2003) and they also provide a potentially useful isotopic system for biogeochemical studies. However, despite the fact that Se is an element of important biologic interest (Stolz and Oremland, 1999), the biologic Se transformation and mobilization in seafloor hydrothermal systems has received little attention.

Although experimental simulation and field studies of Fe and Se isotopes are advancing rapidly, the application of these new isotopic tools as biomarkers remains unclear as abiotic processes can fractionate the isotopes to a similar extent as biotic processes. Equilibrium and kinetic Fe isotopic fractionation between Fe(III) and Fe(II) complexes may produce a large isotopic shift comparable to, or greater than, that produced by microbially-mediated reduction of ferrihydrite (Bullen et al., 2001; Matthews et al., 2001; Johnson et al., 2002). Several workers have also predicted significant equilibrium Fe isotope fractionations based on spectroscopic data for various minerals (Polyakov and Mineev, 2000) and aqueous Fe species (Schauble et al., 2001). Recent field studies of Fe isotope variations in ancient rocks such as in Banded Iron Formations or in Jurassic altered oceanic crust suggested that Fe isotope variations reflect a combination of (1) mineral-specific isotope fractionation (2) variation of the isotope composition of the fluids from which they were precipitated and (3) potential effects of metabolic processing of Fe by bacteria (Johnson et al., 2003; Rouxel et al., 2003). Similarly, kinetic reduction of Se oxyanions by various reducing agents induces much greater isotopic fractionation than does bacterial reduction (Krouse and Thode, 1962; Johnson et al., 1999; Rouxel et al., 2001; Johnson and Bullen, 2003). Although microbial reduction of Se is important, and likely dominant in natural systems (Oremland et al., 1994), recent research has identified abiotic reduction of Se(VI) by green rust as an alternative important process (Myneni et al., 1997), which may induce large Se isotope fractionation (Johnson and Bullen, 2003). In an attempt to unravel some of this complexity, we present here a study of coupled tracers of Fe and Se isotopes with S isotopes. In this study, we aim to investigate the *relative fractionation* between different isotope ratios to evaluate hydrothermal processes and potential biologic processes. The particular geometry of the Lucky Strike hydrothermal field (near the Azores Triple Junction) provides an opportunity to study the influence of subseafloor hydrothermal processes. Lucky Strike is set in a caldera system and overlies an impermeable silica-rich hydrothermally precipitated slab. It has been demonstrated that subsurface processes, such as conductive fluid cooling and mixing with seawater, are of major importance at this field and harbor large microbial communities. In this paper, the chemical, physical and biologic processes in subsurface zones at the Lucky Strike hydrothermal field have been investigated through the studies of mineral assemblages, and the sulfur, selenium and iron isotope compositions. This study provides the first opportunity to link novel isotopic tracers, such as Se and Fe isotopes with S isotopes in the study of hydrothermal systems and to evaluate their use for the search of isotopic tracers of life in extreme environments.

2. GEOLOGICAL SETTING

The Lucky Strike hydrothermal field on the Mid-Atlantic Ridge (MAR) at 37°17′N was discovered in 1992 during dredging operations carried out during the FARA Program (French-American Ridge Atlantic) (Langmuir et al., 1997) and also studied during the European MARFLUX and AMORES projects between 1993 and 1999. The surface extension of the field is one of the largest found in the ocean and the active vents are located around a lava lake of 300 m in diameter located in the central depression between 3 volcanic cones composed of older, highly vesicular volcanic breccia (Fouquet et al., 1994, 1995) (Fig. 1). A unique feature of the Lucky Strike hydrothermal field is the occurrence of layered silicified volcanic deposits termed “hydrothermal slab”. The conductive cooling of the high temperature fluid before mixing with seawater produces sulfide-barite-silica layered formations cementing volcanic breccia. These formations can act as an impermeable lid and enhance subsurface formation of massive sulfides. A large number of active and inactive hydrothermal chimneys have been found at a water depth of 1750 m surrounding the lava lake (Fig. 1). Chimneys and spires grow through these deposits and diffuse, low temperature flow through the cracks in the slab substrate is common. Shimmering water, large populations of hydrothermal vent biota, particularly mussels, and the presence of a white flocculent material, probably bacterial in origin (Langmuir et al., 1997) identify areas of diffuse venting.

The chemical analysis of diffuse hydrothermal fluids circulating within cracks of the slab reveals the presence of less than 7% of a high-temperature hydrothermal end-member (Cooper et al., 2000). Diffuse flows appear to be formed by two mechanisms: (1) conductive heating of seawater; (2) mixing of end-member vent fluid with seawater beneath the hydrothermal slab. The shallow water depth of the Lucky Strike field results in phase separation of the high temperature hydrothermal fluid producing a gas rich vapor phase with low chlorinity (Charlou et al., 2000). Hydrothermal vent fluids are characterized by temperatures ranging from 170 to 324°C, low hydrogen sulfide ($<$3.0 mmol/kg), high Ba concentrations and low metal concentration, and a distinct chemical end-member indicative of a significant geographic control of the venting system (Charlou et al., 2000). The unusual fluid composition at Lucky Strike suggests a deep hydrothermal root zone characterized by a relatively oxic, and previously altered substrate (VonDamm et

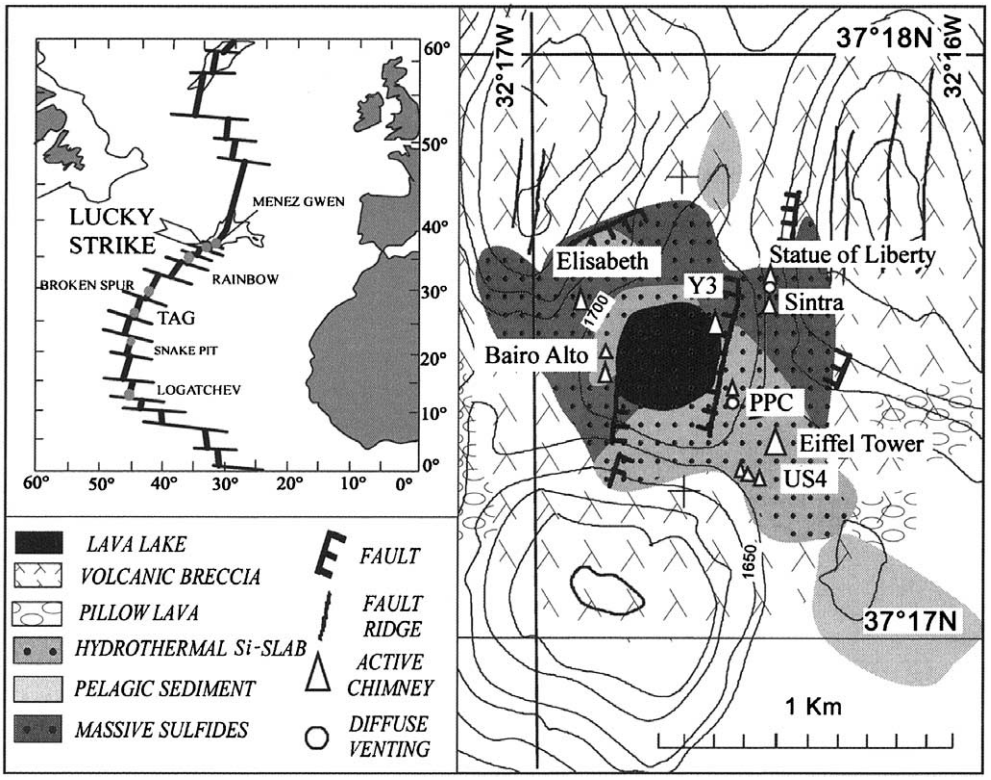

Fig. 1. Geological map of the Lucky Strike hydrothermal field along the Mid-Atlantic Ridge near the Azores Triple Junction. Chimneys studied are shown. After Y. Fouquet (personal communication).

al., 1998; Charlou et al., 2000). Chemical, including metal contents, and temperature variations between vent fluids are mainly due to the combined effect of conductive cooling and mixing with seawater or diffuse flow leading to the deposition of sulfides in subsurface environment.

3. SAMPLES

Massive sulfides and active chimneys from the Lucky Strike field were sampled during the French-American cruise in 1993, DIVA1 (1994) and FLORES (1997) cruises. Reflected and transmitted light microscopy, and electron microprobe analyses were used for mineral identification and textural interpretations. Based on vent structures, mineral abundance and zonation, three types of hydrothermal deposits were identified. The classification is consistent with previous studies of hydrothermal deposits at Lucky Strike (Langmuir et al., 1997). The mineral abundance and texture types are summarized in Table 1. Individual spire complexes include several types of precipitates related to direct high temperature discharge (Type A deposits) and to lower temperature and diffuse flows (Type B and C deposits). In general, Cu-sulfides such as chalcopyrite are characteristic of type A deposits, whereas pyrite and marcasite are highly enriched in type B deposits. Individual samples studied are described in Table 2.

3.1. Type A Deposits (Cu-Rich Deposits)

Active Cu-rich chimneys have mineralogical zonation from chalcopyrite ($CuFeS_2$) on the inner walls to anhydrite on the

Table 1. Characteristics of mineral type and distribution in chimney A, B and C.[a]

	Hydrothermal deposits types		
Mineral type and morphology	Type C	Type B	Type A
Pyrite			
Euhedral (cubic)	tr	xxxx	xxx
Polycrystalline, massive	x	xxx	xx
Colloform, spheroidal (melnicovite)	x	x	
Dendritic	x	x	
Marcasite			
Euhedral (bladed)	tr	xxxx	tr
Polycrystalline, massive	xx	xxx	xx
Colloform, spheroidal	xx	x	x
Dendritic	xx	xxx	xx
Inclusion	tr	x	xx
Sphalerite			
Euhedral, coarse grained	xxxx	x	xxx
Inclusions	xx	xx	xx
Colloform, encrustation	xx	x	x
Chalcopyrite			
Euhedral/subhedral bladed			xxxx
Inclusions	x	x	xx
Anhedral, dendritic		x	
Covellite			
Polycrystalline aggregate			tr
Anhydrite			
Euhedral, acicular			xx
Barite			
Euhedral to dendritic	xxxx	xx	
Silica			
Amorphous, globular	x	xx	tr

[a] tr, trace; x, minor; xx, ubiquitous; xxx, abundant; xxxx, major.

Table 2. Sulfur, selenium, iron isotopic composition, and selenium level of hand-picked hydrothermal minerals.[a]

Sample	Deposit type	Mineral type	$\delta^{34}S$ (‰)	Se (ppm)	$\delta^{82}Se$[b] (‰)	$\delta^{57}Fe$[c] (‰)	Description
Bairo Alto	Group I						
FL-19-08	B	py/mar	0.2	9.7	−4.41	−2.89	Massive pyrite and marcasite aggregate
FL-19-08	B	py/mar	—	—	−4.34	—	
FL-24-01	B	py/mar	0.4	25	−3.63	−1.97	Fine euhedral aggregates of marcasite or
FL-24-01	B	cpy	2.5	869	−2.99	−0.70	chalcopyrite lining large tortuous conduit
FL-24-01 resampled	B	cpy	—	805	−1.95	—	
FL-24-02	B	py/mar	0.1	36	−3.18	−2.92	Flange composed principally of massive
FL-24-02	B	sph	1.2	5.5	−3.60	—	marcasite and dendritic sphalerite in
FL-24-02b	B	sph	1.7	3.0	—	—	internal zone, matrix of barite
FL-29-02	A	cpy	3.9	1340	−2.87	0.29	Chimney with coarse grain lining conduit
Helene	Group I						
DV-19-09	B	py/mar	−0.5	3.6	−3.28	−2.59	Coarse euhedral pyrite filling internal zone
DV-19-09 resampled	B	py/mar	—	—	−3.71	−2.91	of chimney
Elisabeth	Group I						
DV-19-12	C	bar	22.2	0.02	—	—	Euhedral blade of barite in upper zone of Barich slab
FL-24-03	A	cpy	1.5	1460	−2.68	0.51	Thin chimney wall with chalcopyrite lining
FL-24-03	A	cpy	—	—	−2.31		central conduit
FL-29-07A	A	cpy	1.8	430	−3.35	0.10	Porous chimney with number of conduits filled with chalcopyrite
Y3	Group II						
DV-01-05	A	cpy	3.5	960	—	—	Outer zone of chimney massive aggregates
DV-01-05	A	py/mar	2.0	90	−2.84	—	of marcasite and chalcopyrite
DV-01-05	A	cpy	3.9	890	−2.77	—	Euhedral/massive chalcopyrite lining conduit
DV-01-05	A	sph	3.9	106	—	—	and late granular void-fill sphalerite
FL-18-03	C	sph	3.4	1.9	—	—	Granular aggregate sphalerite in internal part of flange
FL-18-04	C	sph	3.6	28	−2.90	−1.06	Large granular aggregate of euhedral sphalerite
FL-21-02	A	cpy	3.9	1130	−2.22	0.35	Thin chimney wall with chalcopyrite lining central conduit
Statue of Liberty	Group II						
ALV-2604-5-1A	C	sph	3.2	1.2	—	—	Barite blades in upper flange zone
ALV-2604-5-1A	C	bar	21.2	—	—	—	
Sintra	Group II						
ALV-2605-3-1	B	py/mar	1.5	1.30	−2.17	−2.97	Massive marcasite intergrowth with barite
ALV-2605-3-1 ditto	B	py/mar	—	—	−2.01	−3.16	
ALV-2606-3-2	B	py/mar	2.9	8.9	−4.24	−2.22	Marcasite blades in chimney conduit
ALV-2606-3-2 ditto	B	py/mar	—	—	−3.90	−2.13	
ALV-2606-4-1J	B	py/mar	2.1	15	−4.09	−1.75	Euhedral blade of marcasite internal flange
ALV-2606-4-1J	B	py/mar	—	—	−3.75	−1.62	zone
DV-09-04	B	py/mar	2.0	20	−3.17	−2.08	Diffuse chimney, flange like composed of
DV-09-04 ditto	B	py/mar	—	—	−2.92	−1.90	blade and porous marcasite
FL-24-04	B	py/mar	3.7	8.3	−4.28	−2.32	Fine euhedral aggregates of marcasite lining
FL-24-04 ditto	B	py/mar	—	—	−4.64	−2.63	large tortuous conduit
Eiffel Tower	GroupIII						
DV-02-01	A	cpy	4.6	1195	−2.48	0.00	Euhedral chalcopyrite filling conduit
DV-02-01	B	py/mar	0.0	10	−4.28	−2.27	Porous chimney with bladed aggregates of
DV-02-01 ditto	B	py/mar	—	—	−4.50	−2.43	marcasite
DV-2	B	py/mar	0.1	30	−5.32	—	Euhedral to fine grain marcasite
DV-2 ditto	B	py/mar	—	—	−5.17	—	
FL-20-04a	A	cpy	4.5	215	−5.49	−0.28	Chalcopyrite lining voids
FL-20-04a resampled	A	cpy	—	161	−6.29	−0.39	
Marker US4	GroupIII						
ALV-2608-2-1	A	cpy	4.6	315	−4.08	0.20	Euhedral to anhedral chalcopyrite filling central chimney conduit
Dredged Samples	Group IV						
FL-DR-03	A	cpy	3.4	435	−1.38	−0.70	
FL-DR-03 resampled	A	cpy	—	—	−1.44	—	Massive sulfide with associated aggregates
FL-DR-03	A	py/mar	1.8	1.6	−1.22	−2.00	of pyrite and chaclopyrite, some void
FL-DR-03 resampled	A	py/mar	—	—	−1.18	−2.70	filled with barite blades
FL-DR-03	A	bar	23.0	0.35	—	—	
FL-DR-03-09	A	cpy	3.3	1160	−1.63	−0.70	Massive sulfide principaly composed by pyrite; Vein of covellite
FL-DR-04-02	A	bar	21.9	0.1	—	—	Massive sulfide with enriched zone of barite
FL-DR-08	A	py/mar	2.0	130	−2.39	−1.85	Massive sulfide composed mostly by pyrite and marcasite, chalcopyrite is minor

Table 2. Continued

Sample	Deposit type	Mineral type	$\delta^{34}S$ (‰)	Se (ppm)	$\delta^{82}Se$[b] (‰)	$\delta^{57}Fe$[c] (‰)	Description
FL-DR-08-1A	A	bn/cov	1.7	54	—	—	Massive sulfide composed mostly by pyrite and marcasite, chalcopyrite is minor; covellite and native sulfur are locally enriched
FL-DR-08-1A	A	py/mar	1.6	245	—	—	
FL-DR-08-1A	A	S	4.1	—	—	—	
FL-DR-08-A	A	py/mar	0.9	4.6	—	—	Massive sulfide composed mostly by pyrite and marcasite; chalcopyrite is minor
Inactif	Group IV						
DV-05-07	A	cpy	2.5	452	−1.65	−0.49	Massive sulfide locally enriched in massive chalcopyrite
DV-05-07	A	py/mar	3.9	158	−1.89	−1.92	
DV-03-04	A	py/mar	1.5	1.6	—	—	Massive sulfide with late void-fill chalcopyrite in ancient conduit and external crust of marcasite
DV-03-04	A	cpy	2.9	448	−3.18	−0.35	
DV-03-04 ditto	A	cpy	—	—	−3.23	—	
FL-19-05	B	py/mar	2.2	27	−1.94	−1.71	Porous zone of chimney composed of massive to fine grains of pyrite with marcasite
DV-05-02-1/2	A	cpy	2.7	340	—	—	Massive sulfide composed of aggregates of coarse grains of pyrite/marcasite with chalcopyrite
DV-05-02-1/2	A	py/mar	1.0	3.3	—	—	
DV-05-02-2/2	A	cpy	1.9	213	−2.15	—	Ancient conduit zone filling with chalcopyrite
FL-18-11	A	cpy	3.1	1640	−1.87	0.20	Massive sulfide coarse grain chalcopyrite
FL-18-11 ditto	A	cpy	—	—	−1.66	0.29	locally altered
Slabs and basalts							
DV-1-2				0.17	−1.29	−0.05	Fresh glass from lava lake
DV-6-2				0.07	−1.34	—	Fresh glass from lava lake
FL-21-03	C	bar	21.3	0.02	—	—	Euhedral blade of barite in upper zone of Barich slab

[a] py, pyrite; mar, marcasite; bar, barite; cpy, chalcopyrite; sph, sphalerite; bn/c, bornite/covelite assemblage; S, native sulfur.
[b] $\delta^{82}Se$:$^{82}Se/^{76}Se$ ratio relative to MERCK standard (Rouxel et al., 2002).
[c] $\delta^{57}Fe$:$^{57}Fe/^{54}Fe$ ratio relative to IRMM-14 international standard.

outer walls. Other minerals are sphalerite (ZnS) and pyrite/marcasite (FeS_2). Marcasite can form an external crust in mature chimneys and Cu-rich massive sulfides, and occurs as microcrystalline grains filling cavities. These deposits are typical black smokers which formed at temperature higher than 300°C. Other black smoker chimneys (e.g., the Y3 vent) were probably characterized by a lower temperature and sphalerite precipitation in the interior of the chimney. The Cu-rich massive sulfides are composed of numerous relics of ancient conduits of black smokers lined with chalcopyrite.

3.2. Type B Deposits (Fe-Ba-Rich Deposits)

The major minerals in Type B deposits are iron disulfides and barite. Barite generally occurs in the outer part of the chimney. These vents emit metal-depleted fluids of lower temperature and at a lower fluid flow velocity. Most of the deposits are porous and are composed of multiple conduits. The shapes range from diffusers to typical chimneys. The diffusers are composed mainly of euhedral marcasite blades up to several mm in length, whereas the chimneys are principally composed of euhedral pyrite cubes up to several mm in size. The inactive edifices are slightly oxidized to Fe-oxides, and the maturation of these deposits is considered to result in the formation of the Fe-rich massive sulfides composed of pyrite with trace amounts of marcasite and chalcopyrite.

3.3. Type C Deposits (Ba-Zn-Rich Flanges)

These horizontal structures are typically located near the base of the spires, and are characterized by enrichment in sphalerite which occurs as euhedral to dendritic minerals in the internal parts of the deposit. The hydrothermal fluid is trapped under the horizontal structure at temperatures between 180°C and 220°C. The upper parts of the horizontal structures of the flanges are also enriched in silica and serve as substrates for biologic activity. Barite forms the matrix of sulfide minerals among which marcasite is the dominant iron sulfide, whereas pyrite is generally a minor mineral. Sphalerite in the Ba-rich samples has low iron content (<2 mol%) which is in accord with a decrease in the temperature of precipitation and/or increase of the sulfur activity (Barton and Toulmin, 1966). Fe-poor sphalerite is also characterized by paragenesis with galena and Cu-sulfosalts similar to enargite (Cu_3AsS_4) and tennantite ($Cu_{12}AsS_{13}$).

4. ANALYTICAL METHODS

For geochemical analysis, mineral separates were prepared by crushing and hand picking under a binocular microscope. Minerals (between 100 mg to 500 mg) were powdered in an agate mortar.

4.1. Sulfur Isotopes

Sulfur isotope analyses were performed on a VG602D double-collector mass spectrometer and are given in conventional $\delta^{34}S$ notation relative to V-CDT (Coplen and Krouse, 1998). The NIST series of

sulfide standards were used for calibration and gave IAEA-S-1 = −0.3‰, IAEA-S-2 = 21.6‰ ± 0.1‰, IAEA-S-3 = −31.6‰ ± 0.1‰, NBS-123 = 17.4‰ ± 0.1‰, NBS-127 = 20.4‰ ± 0.2‰ based on replicate measurements. The precision for sulfide data is typically ± 0.2‰ (2σ level) and is often better than 0.1‰, whereas sulfate isotope data are given at 0.3‰ due to the correction for oxygen mass interference in SO_2 analyses. Individual results are presented in Table 2.

4.2. Selenium Content and Isotopic Composition

Selenium contents (Table 2) were determined by Atomic Absorption Spectrometry following the method described in Marin et al. (2001). Analytical absolute error is typically 10% and the detection limit has been evaluated at 0.02 ppm.

Selenium isotope analyses were performed using a Micromass Isoprobe MC-ICP-MS operating at CRPG-CNRS Nancy, France. The analytical procedures for chemical purification and isotopic analyses are presented in Rouxel et al. (2002) together with preliminary results of Se isotope composition of igneous material and hydrothermal deposits. After chemical purification using thiol cotton fiber, the sample was introduced in the plasma torch using a continuous flow hydride generation system. Instrumental mass bias was corrected using a "standard-sample bracketing" approach. The estimated external precision of the $^{82}Se/^{76}Se$ isotope ratio is 0.25‰ (2σ) for a quantity of Se per analysis as low as 50 ng. For enriched samples (>100 ppm), we used 500 ng of Se for isotopic measurements. The data are reported relative to our internal standards (MERCK elemental standard solution) (Rouxel et al., 2002). Individual $^{82}Se/^{76}Se$ isotope ratio analysis, including various duplicates are presented in Table 2. The $^{82}Se/^{76}Se$ ratio was measured along with the $^{82}Se/^{78}Se$ ratio (Fig. 2a) and Se isotope data fall within the error along the theoretical mass fractionation line suggesting that measurements are not biased by uncorrected interferences.

4.3. Iron Isotopic Composition

Fe isotope ratios were determined using the analytical procedure described in Rouxel et al. (2003) and summarized below.

About 50 mg of samples were dissolved in a mixture of concentrated HCl and HNO_3 acid mixture. The acid solution was taken to dryness at 80°C on a hot plate and dissolved in 5 mL of 8 N HCl by heating at 40°C in closed vessel. A precise volume of this solution corresponding to 2500 μg of Fe was then purified on Bio-Rad AG1-X8 anion resin (VanderWalt et al., 1985). After 20 mL of 8 N HCl was passed through the column to remove the matrix and to elute other ions (such as Cu), 5 mL of 0.12 N HCl was used to elute Fe. The purified samples were then diluted 100-fold (i.e., to 5 ppm) in HNO_3 0.01 N prior analysis by mass spectrometry. Because Fe isotopes can be fractionated during column chromatography (Anbar et al., 2000), we verified that the yield for Fe purification was complete. We measured the Fe concentration in several sample solutions passed through AG1-X8 column in HCl 8 N. Under these conditions, Fe is retained on the resin and the Fe concentration in the eluted solution has been found to be less than 1% of the initial Fe concentration. This suggests that the chemistry yield is better than 99% and does not produce significant isotope fractionation.

$^{57}Fe/^{54}Fe$ ratios were determined with a Micromass Isoprobe MC-ICP-MS operating at CRPG-CNRS Nancy, France. The hexapole collision cell technology of the Isoprobe using a mixture of Ar (at ~1.5 mL/min) and H (at ~0.8 mL/min) results in a decrease of the isobaric interference from ArO^+ and ArN^+ on ^{54}Fe and ^{56}Fe isotopes to a negligible level below 0.1 mV. However, it was found that H enhances the formation of $ArOH^+$ (up to 10 mV) which is highly detrimental for the precise analysis of $^{57}Fe/^{54}Fe$. For routine analysis, we used only Ar as a collision gas (without H) as it was found out that the contribution from ArN^+ and $ArOH^+$ at mass 54 and 57 respectively was typically at 1–5 mV level corresponding to ~0.1 to 0.5% of the Fe ion beams when a solution of Fe at a concentration of 5 ppm is analyzed. Instrumental mass bias was corrected using a "standard-sample-standard" approach and on-peak zero background substraction (Rouxel at al., 2003).

As sample matrix may affect instrumental mass bias or create complex isobaric interferences in the MC-ICP-MS, we verified that a single pass through the ion exchange column was sufficient to reduce sample matrix to the purity of the standard by measuring a standard solution doped with basalt matrix. The Fe concentrations in the synthetic samples have been adjusted at 1 to 2 wt% and Fe isotope compositions have been found to be identical, within uncertainty, to the isotopic composition of the ultra-pure standard solution (Rouxel at al., 2003).

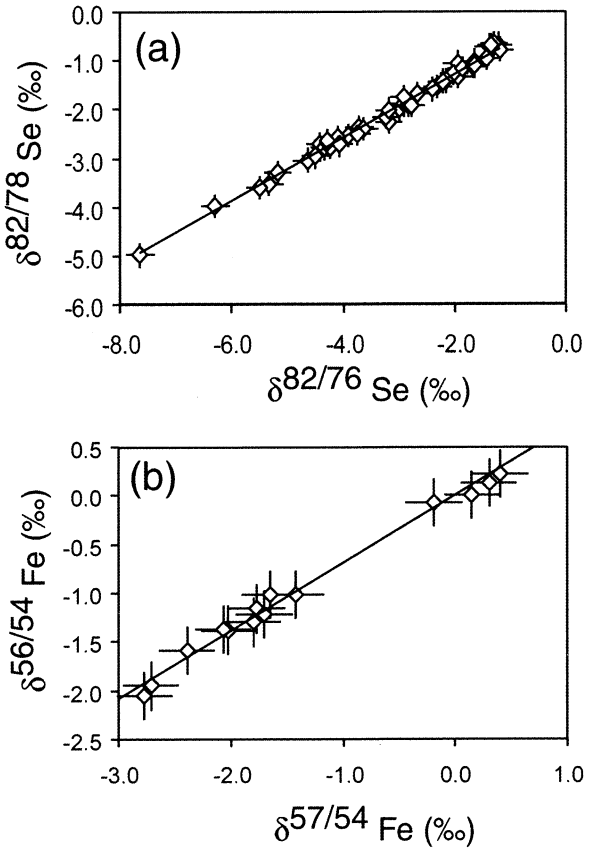

Fig. 2. Correlation of (a) $\delta^{82/78}Se$ and $\delta^{82/76}Se$ and (b) $\delta^{56/54}Fe$ and $\delta^{57/54}Fe$ for a selected suite of samples analyzed in this study. The solid lines correspond to the least-squares regression of the isotopic data, defined by equations (a) $\delta^{82/78}Se = 0.646*\delta^{82/76}Se$ ($r^2 = 0.992$) and (b) $\delta^{56/54}Fe = 0.674 * \delta^{57/54}Fe$ ($r^2 = 989$). These are within error similar to the theoretical relationship for mass-dependent isotopic fractionation.

For selected samples, we also measured the $^{56}Fe/^{54}Fe$ in addition to the $^{57}Fe/^{54}Fe$ isotope ratio as an internal check of the quality of the data. These measurements were made in two different analytical sessions, as the sample concentration used to analyze the $^{56}Fe/^{54}Fe$ ratios do not permit the precise measurement of the $^{57}Fe/^{54}Fe$ ratios. Results are illustrated in Figure 2b and confirm that $^{57}Fe/^{54}Fe$ ratio measurements are not subject to uncorrected isobaric interferences.

Several georeference materials (Govindaraju, 1994) of igneous rocks and the Fe isotope reference standard IRMM-014 have been analyzed for their Fe isotopic composition relative to our internal Fe standard and converted relative to IRMM-14 (Rouxel et al., 2003). We obtained for BIR-1, BR, BE-N, BCR-1, BHVO-1, $\delta^{57}Fe$ values of 0.06‰, 0.12‰, 0.18‰, 0.19‰, 0.23‰ respectively, suggesting that the upper mantle reservoir (i.e., average igneous rocks) has a value of 0.13‰ ± 0.17‰ relative to IRMM-14. This baseline is thus indistinguishable from the average of lunar and terrestrial igneous rocks defined at $\delta^{57}Fe$ = 0.14‰ ± 0.08‰ relative to IRMM-14 by Beard et al. (2003a). All data in this study are hereafter reported relative to the international Fe isotopic standard IRMM-14. Based on duplicate analysis of samples and standard processed through chemistry, we record an external precision of 0.20‰ (2σ level) using this analytical procedure (Rouxel et al., 2003).

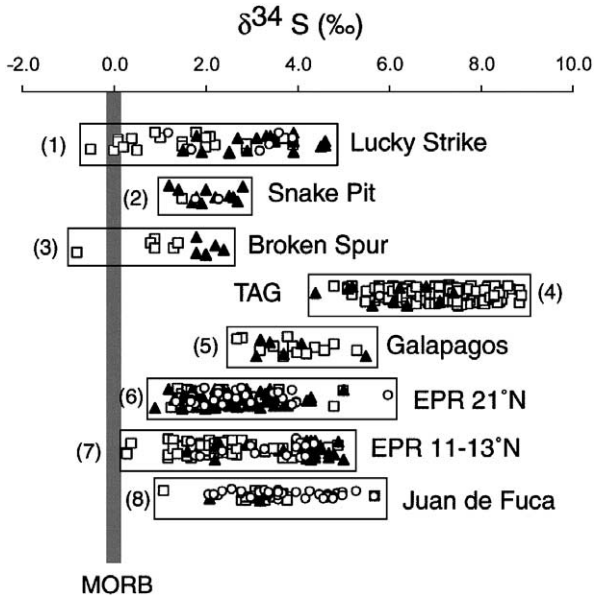

Fig. 3. Sulfur isotope variations in sulfides from different seafloor hydrothermal deposits in unsedimented midocean ridges and back-arc basins. Filled triangle: chalcopyrite; open square: pyrite and marcasite; circle: sphalerite. Reference data for (1) Lucky Strike (this study), (2) Snake Pit (Kase et al., 1990), (3) Broken Spur (Duckworth et al., 1995), (4) TAG (Chiba et al., 1998; Gemmell and Sharpe, 1998; Knott et al., 1998), (5) Galapagos Rift (Skirrow and Coleman, 1982; Knott et al., 1995), (6) EPR 21°N (Arnold and Sheppard, 1981; Styrt et al., 1981; Kerridge et al., 1983; Alt, 1988; Woodruff and Shanks, 1988), (7) EPR 11-13°N (Bluth and Ohmoto, 1988), (8) Juan de Fuca (Shanks and Seyfried, 1987).

5. RESULTS

The $\delta^{34}S$, $\delta^{82}Se$ (i.e., $\delta^{82/76}Se_{MERCK}$), $\delta^{57}Fe$ (i.e., $\delta^{57/54}Fe_{IRMM\text{-}14}$) values and selenium concentrations are presented in Table 2.

5.1. Sulfur Isotopic Composition

The total range of the $\delta^{34}S$ values for 45 sulfide-mineral separates is from −0.5‰ to 4.6‰ with a mean of 2.3‰ and the spread of these values overlaps most of the data for known active chimneys at unsedimented ridges (Fig. 3). However, low $\delta^{34}S$ values at 0‰ ± 1‰ observed at Lucky Strike are not usual for seafloor hydrothermal deposits and are an important characteristic of this field.

The $\delta^{34}S$ for pyrite/marcasite ranges from −0.5‰ to 3.9‰ with a mean of 1.4‰ for 22 samples, whereas for chalcopyrite the values range from 1.9‰ to 4.6‰ and the mean is 3.2‰ for 17 samples. Sphalerite has an intermediate value with a mean of 2.8‰ for 6 samples. Consistent differences are observed between sulfide species, with $\delta^{34}S$ of medium to low temperature pyrite/marcasite assemblage being lower than $\delta^{34}S$ of high temperature chalcopyrite. This difference may be observed within individual specimen (i.e., difference between sulfide pairs), for example in FL-24-01, DV-03-04, DV-02-01, or between sample types within individual chimneys (i.e., difference between type A and type B deposits for the Bairo Alto or the Eiffel Tower vent). There is no simple relationship between the sulfur isotope composition of sulfides and the location of the hydrothermal spires, but the active hydrothermal chimneys tend to have a distinct sulfur isotope signature, with for example chalcopyrite from the Y3 and Eiffel Tower chimneys being heavier than chalcopyrite from the Elisabeth chimney.

5.2. Selenium Content and Isotopic Composition

Selenium levels in different sulfides vary greatly, from 1.2 ppm to 1640 ppm, and different geochemical signatures are recorded both between minerals and between active chimneys. The lower values are observed in marcasite/pyrite and sphalerite with an average of 45 ppm for 22 analyses and 24 ppm for 6 analyses respectively. Chalcopyrite yields the highest value of selenium, with an average of 794 ppm for 17 analyses and the values vary significantly between 213 ppm and 1640 ppm. Sulfates (barite) are characterized by sulfur isotope signatures close to the seawater value (around 21‰) and are highly depleted in Se (below the detection limit of 20 ppb).

Se-rich Cu-sulfides (up to 1600 ppm), Se-depleted Fe-sulfides (down to 1.6 ppm) and basalts have been analyzed for Se isotope compositions and an overall $\delta^{82}Se$ range of 6.0‰ has been obtained (Table 2 and Fig. 4). Terrestrial igneous rocks and iron meteorites have been analyzed in previous studies (Rouxel et al., 2002), permitting the definition of a Bulk Earth reservoir. As already observed for S isotopes, it seems that the mantle and meteorite Se isotopic variations are limited to a small range of less than 0.5‰ yielding a mean $\delta^{82}Se$ of −1.3‰. Our results, combined with previous data**,** suggest that $\delta^{82}Se$ values of hydrothermal sulfides at Lucky Strike are consistently at or below the basalt values (MORB) at −1.5‰. This is in marked contrast with homogeneous $\delta^{82}Se$ values for other hydrothermal fields such as Logatchev and Rainbow (Rouxel et al., 2002) which have $\delta^{82}Se$ values slightly higher or lower than basaltic values (Fig. 4).

Despite the fact that the present state of knowledge on the variability of Se isotopes in natural systems is rather limited, the variability of Se isotopes at Lucky Strike is important and is in the same order of magnitude of experimental biotic or abiotic Se isotope fractionation during selenite or selenate reduction (Fig. 4). In Figure 5, the $\delta^{82}Se$ data are grouped together and are plotted against the Se content of the samples. Both Se-rich sulfides (chalcopyrite) and Se-depleted sulfides (pyrite/marcasite) have $\delta^{82}Se$ values ranging from basaltic values to fractionated values down to −7‰. In general, mature and old massive sulfides have $\delta^{82}Se$ values close to basaltic values whereas active immature vents yield the lowest values. In particular, the Eiffel Tower chimney has the lowest $\delta^{82}Se$ value for chalcopyrite and pyrite/marcasite. In most chimneys, duplicate sampling and analyses of sulfide confirm that selenium isotopes are heterogeneously distributed within chimneys, but no systematic relationship with other geochemical tracers, such as S isotopes, are observed in Figure 6. However, a group of samples having $\delta^{34}S$ near 0‰ is characterized by $\delta^{82}Se$ below basaltic values.

5.3. Iron Isotopic Composition

The $\delta^{57}Fe$ results presented in Table 2 are compared with previous field and experimental studies in Figure 7. The present

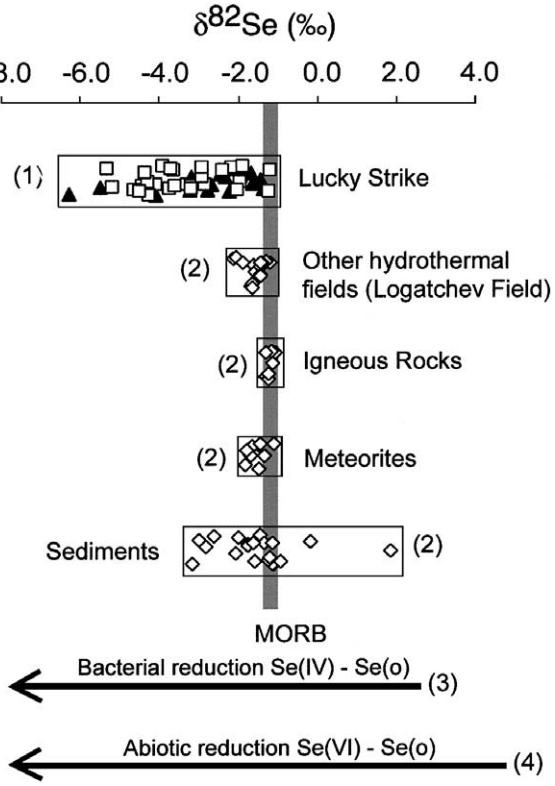

Fig. 4. Diagram showing the distribution of δ^{82}Se in sulfides at the (1) Lucky Strike hydrothermal field (this study) compared with (2) data for meteorites, igneous rocks, sediments and sulfides from Logatchev hydrothermal fields (Rouxel et al., 2002). Results are expressed as per mil deviation relative to the internal standard MERCK. Light grey bar represents the bulk Earth isotopic composition estimated from the composition of igneous rocks and iron meteorites. Se isotope fractionation obtained during (4) chemical partial reduction of Se(IV) to elemental Se (Krouse and Thode, 1962; Rashid and Krouse, 1985) and as observed during (3) bacterial respiratory reduction of selenium oxyanions (Herbel et al., 2000).

results enlarge the δ^{57}Fe range of hydrothermal sulfides studied by Sharma et al. (2001) by more than 2‰. The total spread of the data is around 4‰ which is slightly lower than the total spread observed for ancient sediments such as banded iron formations (Johnson et al., 2003) or during ferrihydrite precipitation (Bullen et al., 2001). However, the data also vary within the range obtained for experimental biologic fractionation (Beard et al., 1999; Brantley et al., 2001) or abiotic fractionation of Fe isotopes between Fe(II) and Fe(III) species (Bullen et al., 2001; Johnson et al., 2002). The most striking feature of the Fe isotope systematics at Lucky Strike field is the relationship between Se content and δ^{57}Fe values for chalcopyrite and pyrite. In Figure 8, the Se and δ^{57}Fe data for active chimneys and massive sulfides, plotted together, define an interesting trend, with Se-rich samples having δ^{57}Fe values close to basaltic value, whereas Se-depleted samples are systematically lighter. As in the case for Se isotopes, no systematic correlation can be drawn by comparing δ^{57}Fe and δ^{34}S values, but sample types form individual groups which do not overlap (Fig. 6). Furthermore, both Fe and Se isotopes are clearly fractionated relative to their basaltic values for samples with δ^{34}S values ~0‰ (Fig. 6), which is a surprising and interesting result (see discussion below).

6. DISCUSSION

6.1. Sulfur Isotope Systematics at Lucky Strike

Petrographical studies have shown that black smokers at Lucky Strike are mineralogically zoned structures reflecting complex growth histories. Massive sulfides presumably represent a very late stage of the maturation of active deposits and are composed largely of fragments of collapsed chimneys. Furthermore, Cu-rich (high temperature, type A deposits) and Cu-poor vents (low temperature, type B deposits) coexist at the same site and the differences in Cu concentration are probably due to subsurface maturation and mixing of vent fluids. At the seafloor, mixing of partially cooled, oxidized and Cu-depleted solutions with seawater results in the precipitation of Fe-poor sphalerite, pyrite and/or marcasite and barite, which are typical of white smoker vents and mounds. Late-stage alteration and mineralization of the deposits is recorded by the mineral assemblages of pyrite-chalcopyrite-bornite and native sulfur-barite void filling in massive sulfides. These secondary minerals, e.g., native sulfur and covellite, have sulfur isotope compositions similar to those of active deposits (Table 2), and suggest that late seafloor processes and weathering do not change the δ^{34}S compositions significantly.

Experimental and theoretical approaches provide models for the behavior of sulfur in seafloor hydrothermal systems (Janecky and Shanks, 1988; Shanks, 2001) and suggest that H_2S in the reaction zone released to the hydrothermal system has an isotopic value of 1 to 1.5‰. The finite reducing potential of the hydrothermal fluid can account for the δ^{34}S variations of 1.5 to 4.5‰ and a further increase in δ^{34}S could result from sulfate reduction involving fresh basalt. At Lucky Strike, our results

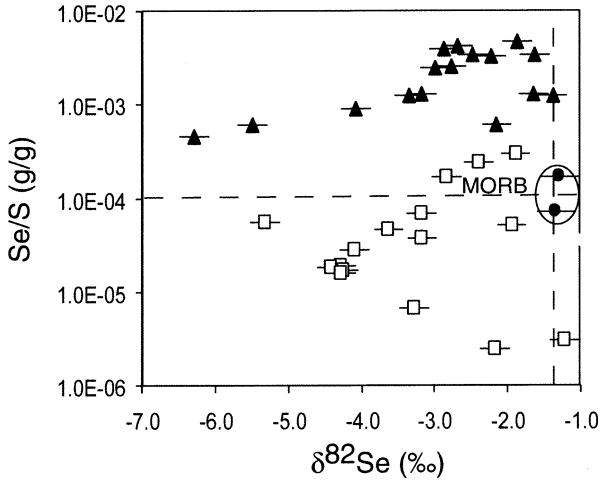

Fig. 5. Se/S ratio and δ^{82}Se values of chalcopyrite (filled triangle), pyrite/marcasite (open square) and basalt (filled circle). Chalcopyrite has Se/S ratios greater than basalts whereas pyrite may have Se/S values greater or below basaltic values. Se/S determined on the basis of stoichiometric formulae of the sulfides and expressed in g/g. For all range of Se/S values, most of sulfides show enrichment in light Se isotopes relative to basalts. Dashed horizontal and vertical lines correspond to midocean ridge basalt (MORB) composition.

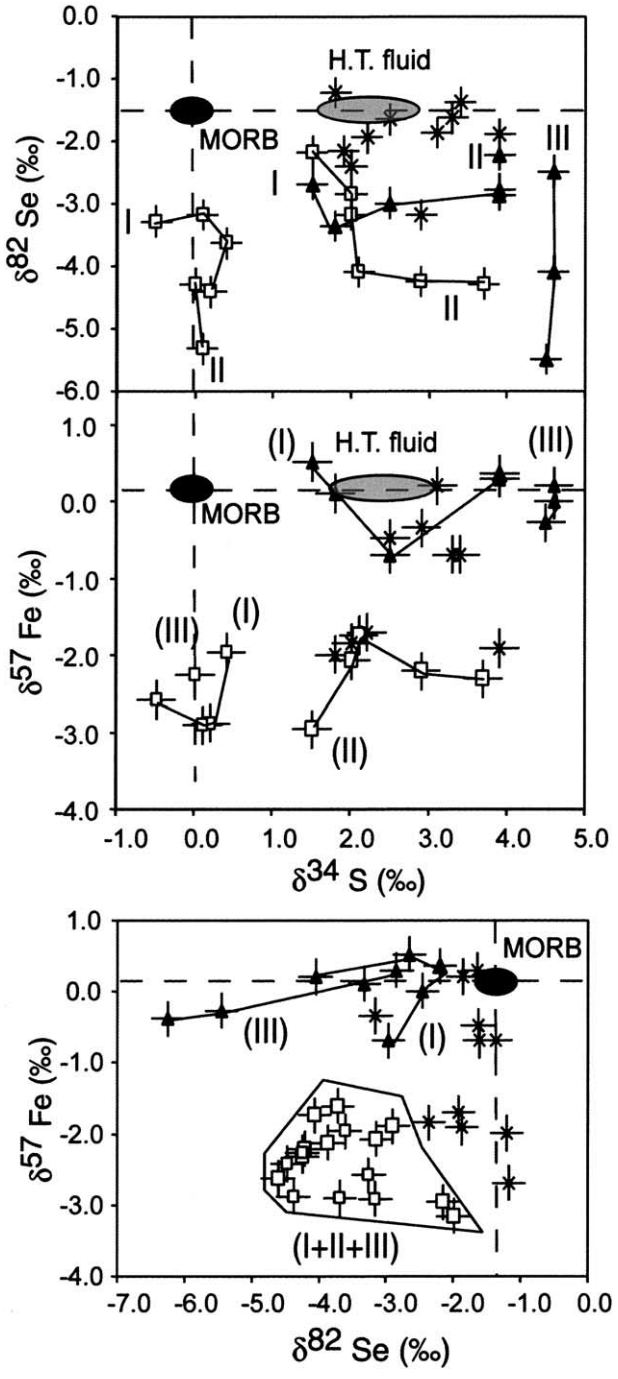

Fig. 6. δ^{57}Fe vs. δ^{34}S, δ^{82}Se vs. δ^{34}S and δ^{57}Fe vs. δ^{82}Se plots for chalcopyrite (filled triangle) and pyrite (open square) from active vents and massive sulfides (crosses). Positions of basaltic and high temperature (H.T.) hydrothermal fluid (i.e., assumed end-member) are shown. Samples are grouped together following their fluid chemistry end-members and geographic location as defined by (Charlou et al., 2000). Group I: N-W vents (Bairo Alto, Elisabeth and Helene); Group II: N-E Vents (Y3, Sintra, Statue of Liberty); Group III: S-SE vents (Eiffel Tower, US4) Group IV: Inactive vents and massive sulfides. Dashed horizontal and vertical lines correspond to midocean ridge basalt (MORB) composition.

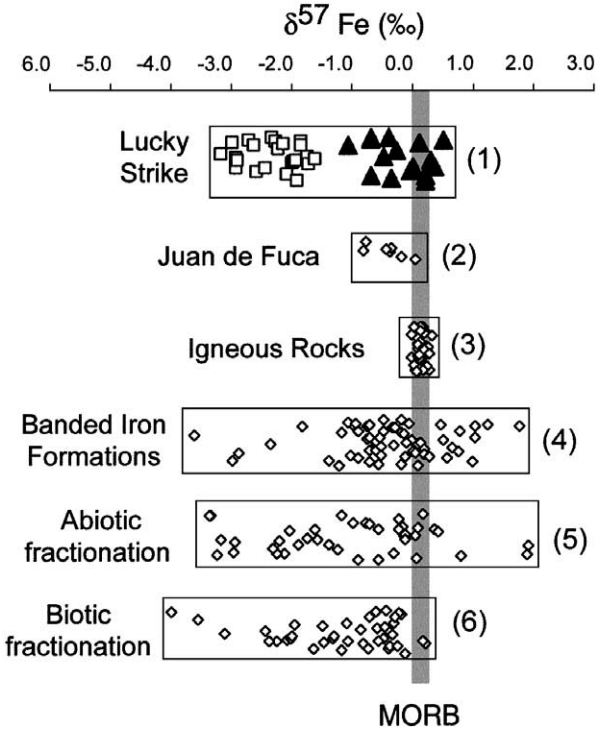

Fig. 7. Diagram showing the distribution of δ^{57}Fe in (1) sulfides at Lucky Strike hydrothermal field (this study) for chalcopyrite (filled triangle) and pyrite (open square). The results are compared with literature data for (2) hydrothermal fluids and sulfides at Juan de Fuca(Sharma et al., 2001), (3) igneous rocks (Beard et al., 2003a) and (4) banded iron formations (Johnson et al., 2003). Results are expressed as per mil deviation of the ^{57}Fe/^{54}Fe ratio relative to the international standard IRMM-14. Light grey bar represents the basaltic composition estimated from the composition of igneous rocks (Beard et al., 2003a; Rouxel et al., 2003). Fe isotope fractionations obtained (5) during abiotic ferrhydrite precipitation (Bullen et al., 2001) and equilibrium Fe(II)-Fe(III) fractionation (Johnson et al., 2001) and (6) from biologic experiments (Beard et al., 1999; Brantley et al., 2001) are also shown for comparison.

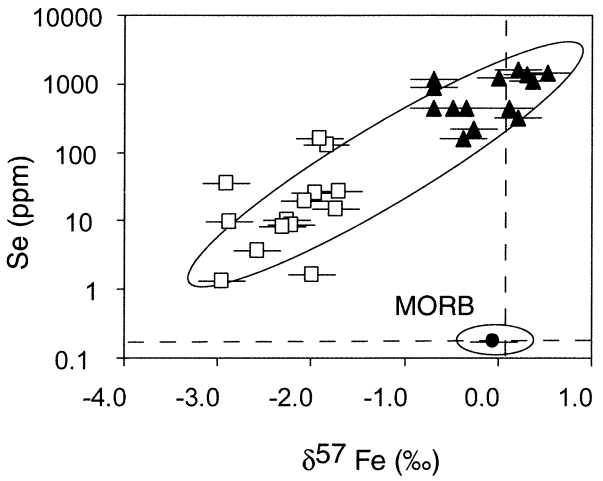

Fig. 8. Se content and δ^{57}Fe values of chalcopyrite (filled triangle), pyrite/marcasite (open square) and basalt (filled circle). Chalcopyrite enriched in Se have δ^{57}Fe close to basaltic value whereas pyrite with lower Se content have δ^{57}Fe values fractionated relative to basaltic value. Dashed horizontal and vertical lines correspond to midocean ridge basalt (MORB) composition.

indicate that the $\delta^{34}S$ values of pyrite/marcasite, in particular for Bairo Alto and Eiffel Tower, tend to be lower than those of chalcopyrite (by 1 to 3‰). The equilibrium isotopic fractionation factor (α) of one sulfide (e.g., chalcopyrite) species with respect to another (e.g., pyrite) is a function of temperature (Ohmoto and Goldhaber, 1997) and the $\delta^{34}S$ of pyrite is higher (by ~1‰) than that of chalcopyrite at the temperatures of hydrothermal systems (250–300°C). Thus, our results indicate a strong isotopic disequilibrium between the pyrite and chalcopyrite, which suggest that they were not cogenetic or coprecipitated. Disequilibrium between sulfide species in hydrothermal systems has been extensively reported and is supported by sulfur isotope studies, and textural relationships between sulfides (Kerridge et al., 1983; Duckworth et al., 1995). The origin of the disequilibrium is not straightforward and may reflect multiple episodes of precipitation, dissolution and replacement of sulfides over a wide range of conditions which are largely dependent on cooling of the fluid and mixing with seawater during venting. At Lucky Strike, the difference in $\delta^{34}S$ between Fe-rich sulfide and Cu-rich sulfide is best explained by considering that Fe-sulfide and Cu-sulfides formed from modified hydrothermal fluids: (i) a metal-depleted (i.e., Cu-poor) low temperature fluid with $\delta^{34}S$ around 0‰; (ii) a high temperature metal-rich (i.e., Cu-rich) fluid with $\delta^{34}S > 1.5$‰.

The $\delta^{34}S$ values of Cu-sulfides from active chimneys (e.g., Y3 and Eiffel Tower) display some increase in $\delta^{34}S$ up to 4.6‰. During high temperature fluid interaction with seawater in a near surface zone, sulfate reduction occurs and this process can shift the $\delta^{34}S$ fluid values from 1.5‰ to 4.5‰ during venting (Janecky and Shanks, 1988).

The $\delta^{34}S$ values obtained for pyrite (down to −0.5‰) are among the lowest values obtained for seafloor hydrothermal deposits in nonsedimented mid oceanic ridges. Low $\delta^{34}S$ values (around 0‰) have been reported from Snake Pit (Kase et al., 1990) and Broken Spur (Duckworth et al., 1995) on the Mid Atlantic Ridge and have been related to a smaller contribution of seawater sulfate to the deposit. At Lucky Strike, low $\delta^{34}S$ values are observed only for low-temperature sulfides (<250°C) precipitated from a hydrothermal fluid which has probably interacted with seawater, precluding quantitative sulfate reduction in the chimney environment. However, because Sr isotope data of vent fluids suggest a significant contribution of seawater in the reaction zone (Bach and Humphris, 1999), the argument that $\delta^{34}S$ around 0‰ represents the direct contribution of magmatic sulfur leached from basalt without interactions with seawater is not applicable and is in disagreement with Se and Fe isotope data as presented in Figure 6 and discussed below.

Low $\delta^{34}S$ values obtained at Lucky Strike cannot be explained by the mixing of hydrothermal fluid ($\delta^{34}S \approx 1.5$‰, Janecky and Shanks, 1988) with reduced seawater sulfates ($\delta^{34}S = 21$‰) and another explanation is thus required. There are several models, discussed below, which may explain why the $\delta^{34}S$ of pyrite is lower than that of chalcopyrite and/or lower than the typical hydrothermal values of around 1.5‰.

(1) A reservoir effect is induced by removal of sulfides by precipitation during cooling of the high temperature fluid and mixing with seawater. As early precipitating sulfides are high-temperature minerals such as chalcopyrite, having a fractionation factor close to zero or slightly negative (Ohmoto and Goldhaber, 1997), this process cannot produce the apparent decrease in $\delta^{34}S$ of the remaining H_2S in the fluid.

(2) A second model would involve the isotopic fractionation of H_2S-bearing hydrothermal fluids during partial oxidation. Partial oxidation of hydrothermal fluids has been observed during boiling processes in epithermal systems (Valles Caldera, New Mexico, McKibben and Eldridge, 1990). It involves the loss of H_2 and H_2S to the vapor phase, causing an increase in the oxidation state of the residual fluid. Mechanisms of partial H_2S-oxidation would produce isotopically lighter hydrothermal H_2S due to the large isotopic fractionation between H_2S and SO_4^{2-}, i.e., preferential oxidation of $H_2{}^{34}S$. Because the fluid chemistry at Lucky Strike is strongly influenced by phase separation with low chlorinity (Charlou et al., 2000), boiling processes may favor isotopic fractionation at depth, i.e., between the reaction zone and surface, but cannot explain the subsurface processes producing the heterogenity in $\delta^{34}S$ observed between and within vents. Furthermore, sulfate which is produced by oxidation of sulfide has $\delta^{34}S$ values essentially identical to those of the initial sulfide (Ohmoto and Goldhaber, 1997).

(3) Partial reduction of seawater sulfate can occur during mixing of the hydrothermal fluid with seawater. At high temperature (250°C-350°C), sulfate reduction during seawater interaction with basalt is a near equilibrium process for sulfur isotope fractionation between the sulfate-reactant and sulfide-product (Shanks et al., 1981). Mechanisms of partial SO_4^{2-} reduction during mixing of the hydrothermal fluid with seawater imply isotopically lighter hydrothermal H_2S due to the large isotopic fractionation between H_2S and SO_4^{2-}, i.e., preferential reduction of $^{32}SO_4^{2-}$. At temperatures greater than 250°C, isotope exchange equilibration between H_2S and sulfate is expected with a fractionation factor of less than 25‰ (Ohmoto and Goldhaber, 1997). The end-member H_2S concentration of hydrothermal fluids at Lucky Strike is between 2.1 mmol and 3 mmol (Charlou et al., 2000). Assuming that all H_2S in the fluid is derived from partial reduction of seawater sulfate ($\delta^{34}S = 21$‰ and $SO_4^{2-} = 9$ mmol/kg after anhydrite precipitation, Shanks et al., 1981) following a single stage Rayleigh distillation, the $\delta^{34}S$ of H_2S produced should be between −1.3‰ and 0.3‰. Although these values are compatible with low $\delta^{34}S$ of pyrite/marcasite, the requirement that more than 90% of the hydrothermal fluid is composed of seawater is not compatible with physicochemical parameters of the fluids. Furthermore, because sulfate reduction is likely to be a near quantitative process in seafloor hydrothermal systems at temperature higher than 250°C (Shanks et al., 1981), the $\delta^{34}S$ value of H_2S produced should be identical to the initial seawater SO_4^{2-}. At lower temperature, kinetic S isotope fractionation may also occur during abiotic reduction of seawater sulfate. Experimental work has identified a significant S isotope fractionation during abiotic reduction which is ~15‰ at 150°C, 10‰ at 200°C and decreasing further with increasing temperature (Machel et al., 1995). In such case, inorganic reduction of seawater sulfate at 21‰ cannot account for $\delta^{34}S$ values of H_2S around 0‰.

(4) The sulfides with low $\delta^{34}S$ were precipitated from hydrothermal fluids containing a small proportion of H_2S derived from bacterial seawater sulfate reduction. Low $\delta^{34}S$ values of sulfides are recorded in active vents, at temperatures higher

than 200°C, which is greater than the maximum temperature supported by thermophiles (Deming and Baross, 1993). Thus in situ bacterial sulfate reduction is not likely to occur in chimney and flange environments. McCollom and Shock (1997) developed thermodynamic models which provide geochemical constraints on the amount of metabolic energy potentially available from chemosynthetic reactions during mixing of hydrothermal fluids with seawater. From their study, it is argued that, because sulfate reduction by chemolithotrophic microbes is limited by hydrogen, a significant proportion of biologically generated H_2S in diffuse flows may mix with the hydrothermal fluid. At Lucky Strike, the concentration of H_2 in hydrothermal endmember fluids is found to be up to 727 μmol/kg (Charlou et al., 2000) and a maximum of 180 μmol of H_2S that may be produced by biologic chemosynthesis in the hydrothermal fluid can be calculated following the approach of McCollum and Shock (1997). Considering that the H_2S concentrations in the fluids vary between 2.1 and 3.0 mmol/kg (Charlou et al., 2000), the proportion of H_2S which may be biogenic would be between 6 to 8%. The sulfur isotope ratios of H_2S that originate from bacterial sulfate reduction could be ~15‰ to 40‰ lighter than their parent sulfate depending on the specific types of bacteria involved and the growth conditions (Canfield, 2001). The resulting sulfur isotope fractionation can be even larger, if intermediate compounds such as thiosulfate or polysulfides are formed (Habicht et al., 1998). Therefore, the resulting composite fluid may have $\delta^{34}S$ values of 1‰ to −0.5‰, considering an initial value of 1.5‰. This may explain the low $\delta^{34}S$ values as low as −0.5‰ observed at Lucky Strikes. McCollum and Shock (1997) suggested that subsurface microbial population is probably a net sink of H_2 due to chemosynthesis and may even quantitatively exhaust the H_2 from hydrothermal fluids in mixing environments. The great variability of H_2 from 3.3 to 727 μmol/kg between vents at Lucky Strike (Charlou et al., 2000) confirms this assumption. Furthermore, small amounts of ammonium were found in the Lucky Strike fluids indicating reaction with a small amount of organic matter below the seafloor (VonDamm et al., 1998). This suggests that an additional source of H_2S from heterotrophic sulfate reducers can contribute to biogenic H_2S fraction.

6.2. Hydrothermal Geochemistry of Selenium Isotopes

Selenium has similar chemical properties to sulfur and substitutes for sulfur in many sulfide minerals. Se follows sulfur in magmatic cycles and is concentrated in magmatic-hydrothermal ores, being richer in the high-temperature deposits (Leutwein, 1972; Auclair et al., 1987). Determination of Se/S ratios in sulfide minerals from massive sulfide ores should thus provide information concerning the origin of Se and S, because the Se/S of seawater differs dramatically from the Se/S ratio of igneous rocks. However, difficulties in using Se as a source indicator are encountered because Se levels in hydrothermal sulfide minerals are highly variable (Auclair et al., 1987), and variations are controlled by parameters other than source effects. The variation of Se contents in hydrothermal chimneys and mounds may be explained principally in terms of the temperature of crystallization of Cu-rich deposits. At 21°N, selenium enrichments correlate positively with sulfur isotopes and suggest seawater sulfate reduction at high temperature (Chaussidon et al., 1991). At 13°N, high Se values, i.e., up to 2500 ppm, occur in high-temperature mineral assemblages in the middle part of the deposit (Auclair et al., 1987). Huston et al. (1995) reported Se contents of pyrite in volcanic-hosted massive sulfide deposits which vary from low levels (<5 ppm) in Cu-poor and Zn-rich deposits, to high values (200 ppm) in Cu-rich deposits. These variations can be best explained by differences in the Se/S of the hydrothermal fluid, rather than by temperature changes. Variations of Se in hydrothermal deposits can thus be caused by: (1) temperature dependent fractionation between coexisting sulfides (Bethke and Barton, 1971; Yamamoto et al., 1984), (2) fractionation controlled by pH, temperature and oxidation state of the hydrothermal fluid (Tischendorf and Ungethüm, 1964; Yamamoto, 1976; Huston et al., 1995), (3) changes of the selenium content of the hydrothermal fluids during sulfide precipitation or mixing with seawater (Huston et al., 1995).

Present-day seawater has a Se/S (g/g) ratio of 6.3×10^{-8} whereas MORB has a Se/S ratio around 1.5×10^{-4}. Thus, Se in barite (Se/S ratio of $\sim 10^{-7}$) at Lucky Strike is derived from seawater, whereas chalcopyrite with a Se/S ratio of 4.7×10^{-3} reflects a dominant contribution from magmatic sources. Sulfur isotope values are consistent with these results. In contrast, pyrite and marcasite, with $\delta^{34}S$ values near 0‰, have global molar Se/S ratios down to 10^{-6} which argues against a magmatic source. In fact, Se levels of pyrite at Lucky Strike are unusually low compared to the Se level of chalcopyrite. The mean partition coefficient of Se at Lucky Strike between chalcopyrite and pyrite is around 30, whereas the partition of Se between coprecipitated pyrite and chalcopyrite has been defined around 4 (Yamamoto et al., 1983). This confirms that pyrite and chalcopyrite formed from distinct hydrothermal fluids having different Se concentrations.

Se in hydrothermal sulfides has a significant range of Se isotopic composition (up to 7‰) which confirms the early experimental and theoretical studies of Krouse and Thode (1962) showing that Se isotopes may vary in nature by more than 10‰. These variations may reflect not only a contribution from different Se-sources but also mass-dependent, kinetic fractionation occurring at low temperatures in aqueous media. In the same way as for S isotopes, Se isotope fractionation in hydrothermal environments is likely to result from complex processes at low temperature such as redox changes, seawater-rock interaction and biologic activity.

As Se is removed during the ascent of the fluid, it is possible that the enrichment in the light isotope in the depleted sample is the result of isotopic partitioning between Se dissolved species and precipitating sulfides. However, because the Se isotopic fractionation factor between the fluid and the precipitated sulfide is likely to be very small under hydrothermal conditions (as for S isotopes), and because no relationship between Se content and $\delta^{82}Se$ values is observed (Fig. 5), we do not favor such processes to explain the variability of $\delta^{82}Se$ observed in hydrothermal sulfides.

Seawater mixing may also explain part of the variations observed, but the Se isotopic composition of seawater must be defined to quantify this effect. Se exists in deep sea water as Se(IV) and Se(VI) oxyanions and, among other characteristics, these two valences have a distinctly different behavior with respect to adsorption on particles. To date no isotopic compo-

sition of these species in seawater has been reported, however, based on the isotopic composition of a Mn-nodule which has a δ^{82}Se value of −1.5‰ (Rouxel et al., 2002) there is no evidence that seawater is significantly fractionated relative to the basaltic value. The large range and highly negative values of hydrothermal deposits observed cannot be explained by simple mixing of Se leached from igneous rock and Se derived from seawater. Johnson et al. (1999) reported measurements of Se isotope fractionation during selenate reduction, selenite sorption, and oxidation of reduced Se. These results, combined with previous studies performed by Rashid and Krouse (1985) indicate that reduction of soluble oxyanions is the major source of Se isotope fractionation. Therefore, based on current knowledge of Se isotope fractionation, we conclude that partial reduction of Se oxyanions (selenate and selenite) must occur at Lucky Strike. As the Se/S ratio of seawater is very low compared to the Se/S ratio of basalt or hydrothermal fluid, partial reduction of seawater Se oxyanions during mixing cannot account for the δ^{82}Se variability in pyrite or chalcopyrite. Furthermore, under hydrothermal conditions, reduction of Se oxyanions is likely to be quantitative as for sulfate reduction.

We interpret the δ^{82}Se variability as a result of leaching and mixing of a fractionated Se source beneath hydrothermal chimneys with the hydrothermal fluid. For one single vent (Bairo Alto) we observed variations up to 4‰ for S isotopes and 3‰ for Se isotopes. This indicates two sources for S and Se which are: (1) the "end-member" hydrothermal fluid with Bulk Earth Se isotopic values (−1.5‰) and typical hydrothermal values at 1.5‰ for S isotopes; (2) a fractionated source hosted in subsurface environment with sulfur at negative δ^{34}S values and Se possibly derived from reduction-enrichment of Se from seawater.

Fluid cooling and mixing with seawater in the subsurface environment provide suitable conditions for microbial activity which may affect Se isotopes. However, abiotic fractionation of Se isotopes during reduction of Se(IV,VI) to Se(0) has been reported and kinetic fractionation of more than 15‰ has been described using reduction by NH_2OH (Krouse and Thode, 1962; Rashid and Krouse, 1985), ascorbic acid ($C_6H_8O_6$) (Rees and Thode, 1966), KI (Rouxel et al., 2001) and Fe(II,III) hydroxide-sulfate (Johnson and Bullen, 2003). Among reducing agents of major importance in suboxic environment, such as subsurface hydrothermal systems, Fe(II,III) oxides may precipitate hydrothermally (Boyd and Scott, 2001) and may be involved in the reduction and immobilization of aqueous Se oxyanions (Myneni et al., 1997).

The subsurface hydrothermal system at Lucky Strike is believed to be fed by conductively heated seawater forming a shallow short-pass hydrothermal convection system (Cooper et al., 2000). The interaction of this diffuse flow with high temperature hydrothermal fluids results in precipitation of sulfides at depth. This suggests circulation of seawater-derived fluid for protracted periods, permitting the preconcentration of reduced Se species in contact with Fe-oxides, with Se oxyanions likely derived from seawater or oxidized sulfides.

The reactivation of this fractionated Se source (probably with δ^{82}Se below −15‰) by the hydrothermal fluid provides the most likely explanation of the δ^{82}Se variation at Lucky strike and probably at other hydrothermal fields (Rouxel et al., 2002). At this stage of our knowledge, it is tempting to dismiss the possibility of bacterial mediation in Se preconcentration and isotopic fractionation. Clearly, the study of Se interactions with deep-sea vent microorganisms is required to clarify whether Se isotopes provide biosignatures of seafloor hydrothermal systems.

6.3. Fractionation of Iron Isotopes in Seafloor Hydrothermal Systems

Fe isotope data for high temperature hydrothermal fluids and sulfides have been reported from hot springs along the Juan de Fuca Ridge (Sharma et al., 2001) and East Pacific Rise (Beard et al., 2003b) and the results suggest that the hydrothermal fluids are lighter by ~0.5‰ to 1‰ relative to basaltic δ^{57}Fe values. An Fe isotope analysis of hydrothermal solution from Lucky Strike has been also reported (δ^{57}Fe value of −0.6‰, Beard et al., 2003b). The δ^{57}Fe values obtained for high temperature chalcopyrite, with variability of less than 1‰, are consistent with previous studies. However, lower temperature sulfides, and in particular Se-depleted pyrite, are depleted in ^{57}Fe (Fig. 8).

The key to inferring the Fe isotope fractionation in seafloor hydrothermal system lies in accurate mineral-fluid isotope fractionation factors, and in particular for pyrite- and chalcopyrite-fluid pairs. The important question, relevant to the interpretation of the difference between δ^{57}Fe values between pyrite and chalcopyrite, is whether the Fe isotope fractionation observed is the result of different equilibrium fractionation factor between pyrite and chalcopyrite, as a result of either temperature changes or mineralogical effects. Using the calculated reduced partition function ratios for pyrite (Polyakov and Mineev, 2000) and hexaquo species (Schauble et al., 2001), it is possible to calculate the δ^{57}Fe values of Fe(II) that might have been in equilibrium with pyrite, assuming a temperature range, for example, between 350°C and 200°C (range of temperature of hydrothermal fluids observed at Lucky Strike). As already found by Sharma et al. (2001), the calculated fractionation factor between Fe(II) and pyrite should be ~1.5‰ at 350°C and ~4‰ at 200°C (^{57}Fe/^{54}Fe ratio). Although experimental investigations are still needed, these theoretical calculations may be, to a first approximation, suitable for predicting the sign of Fe isotope fractionation between fluids and minerals. These calculations indicate a preferential partitioning of the heavy isotope in pyrite. Furthermore, because equilibrium isotopic fractionation is a function of the covalence of the chemical bonds (Polyakov and Mineev, 2000), no large isotopic fractionation should be observed between pyrite and chalcopyrite. Therefore, the Fe isotope composition of pyrite samples at Lucky Strike (both the negative δ^{57}Fe values and the lower values relative to chalcopyrite) is inconsistent with a simple equilibrium fluid-mineral fractionation.

Because the variation in δ^{57}Fe values of pyrite and chalcopyrite follows globally the Se concentration, we suggest that the process depleting Se from the hydrothermal fluid may also fractionate Fe isotopes. As Se geochemistry in seafloor hydrothermal systems is sensitive to sulfide precipitation which readily scavenges Se from the fluid, the effect of subsurface precipitation on Fe isotope fractionation may be evaluated theoretically.

The partitioning of Se between a hydrothermal fluid and iron

disulfide minerals such as pyrite or chalcopyrite is governed by the following general reaction:

$$FeS_2 + 2H_2Se = FeSe_2 + 2H_2S \quad (1)$$

Similarly, the partitioning of Fe isotopes between a hydrothermal fluid and iron disulfide minerals such as pyrite or chalcopyrite is governed by the following general reaction:

$$^{57}FeS_2 + {}^{54}Fe^{2+}_{aq} = {}^{54}FeS_2 + {}^{57}Fe^{2+}_{aq} \quad (2)$$

The reservoir effects on the Fe isotopic ratio and selenium content of the fluid during sulfide precipitation can be modeled by a distillation process and are given by the equation:

$$\delta^{57}Fe_{fluid} = (\delta^{57}Fe_i + 1000)*f_{Fe}^{(\alpha-1)} - 1000 \quad (3)$$

$$(Se/S)_{fluid} = (Se/S)_i*f_s^{(K-1)} \quad (4)$$

where f_S and f_{Fe} are the fraction of H_2S and Fe^{2+} remaining in the fluid respectively. α and K are the isotopic fractionation factors between Fe dissolved complexes and FeS_2 and the partition coefficient of Se between FeS_2 (or $CuFeS_2$) and H_2S. $\delta^{57}Fe_i$ and $(Se/S)_i$ represent the initial values for the undepleted hydrothermal fluid. For disulfide precipitation, f_S and f_{Fe} are dependent factors, linked by the relation:

$$f_{Fe} = 1 - (1 - f_s)*(S/Fe)_i/2 \quad (5)$$

$(S/Fe)_i$ being the initial S/Fe molar ratio of the fluid.

The Se/S ratio in end-member hydrothermal fluid (i.e., Se/S_i) is not well established due to the scarcity of selenium analyses. The most reliable data are given in VonDamm et al. (1985) for vents at 21°N, yielding a $(Se/S)_{fluid}$ ratio of around 10^{-5}. However, these data are probably biased due to some depletion of the fluid before venting (VonDamm et al., 1985). If we assume that Se/S ratio is conservative during basalt alteration at high temperature in the reaction zone, the fractionation factor K_{cpy} must be >20 to produce Se contents of chimney chalcopyrite of up to 1500 ppm. K_{cpy}/K_{py} is considered to be ~4 following the study of Yamamoto et al. (1983) and leads to the assumption that K_{py} is around 5. Iron concentrations in end-members at Lucky Strike are highly variable and low compared to values found in fluids from other hydrothermal areas (Charlou et al., 2000). The initial S/Fe molar ratio of the fluid has thus been inferred based on the highest iron concentration found at Lucky Strike, such as Y3 sites (863 μmol/kg for Fe and 3.0 mmol/kg for H_2S, Charlou et al., 2000).

Using the Fe isotopic composition and the Se content of chalcopyrite and pyrite/marcasite at Lucky Strike, we calculate the theoretical fluid composition in equilibrium with sulfides, using the parameters defined above. The data are plotted in Figure 9, which illustrates pathways of sulfide precipitation. Fe isotopes and Se concentrations of the FeS_2-$CuFeS_2$ sulfide pairs at Lucky Strike are best modeled by pathways with K ranging from 4 to 9 and α assumed at 1.0015.

As estimated above, the calculated isotope fractionation factor α between FeS_2 and $FeCl_4^{2-}$ or $Fe(H_2O)_6^{2+}$ is ~1.0015 at 350°C and ~1.002 at 250°C. Furthermore, the $\delta^{57}Fe$ value of −0.6‰ measured in high-temperature fluid at Lucky Strike (Beard et al., 2003b) is 1‰ lighter than the $\delta^{57}Fe$ value obtained for chalcopyrite ($\delta^{57}Fe$ value up to 0.5‰). The parameters used for modeling Se/S vs. $\delta^{57}Fe$ are therefore consistent

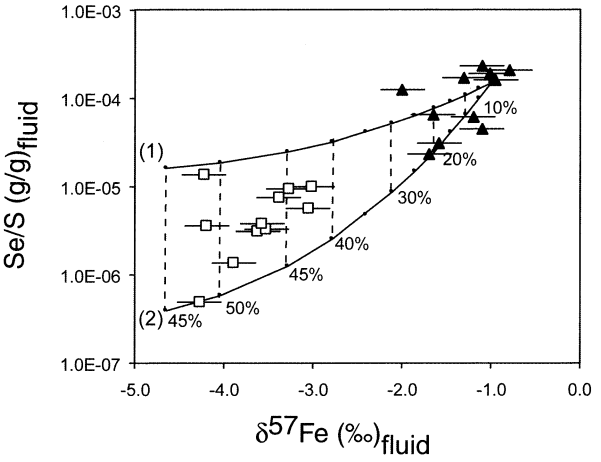

Fig. 9. Calculated Fe isotopic values versus Se/S (weight ratio) of hydrothermal fluid in equilibrium with chalcopyrite (filled triangle) and pyrite (open square) at Lucky Strike. $\delta^{57}Fe$ values are calculated using isotope fractionation factor at α = 1.0015 (pyrite and chalcopyrite). Selenium partitioning factors between the fluid and chalcopyrite or pyrite are assumed to be 20 and 5 respectively. Solid lines illustrate pathways for subsurface sulfide precipitation and the percentages correspond to the degree of H_2S depletion. Pathway 1 is calculated using α = 1.0015 and K = 4. Pathway 2 is calculated using α = 1.0015 and K = 9. See text for definition and discussion.

with the precipitation of $CuFeS_2$ and/or FeS_2 in subsurface environment. The maximum depletion in H_2S in the fluid is constrained to be around 50% which is compatible with the fact that the fluids forming Type B deposits are metal depleted. This is also consistent with high-temperature fluid studies, with for example, H_2S concentration in Eiffel Tower vent fluid changing from 3.29 mmol/kg to 1.78 mmol/kg between 1993 and 1996 (VonDamm et al., 1998).

6.4. S-Se-Fe Isotope Systematics of Seafloor Hydrothermal Systems

The deposit at Lucky Strike formed from different fluids that underwent conductive cooling under the silicified slab, mixing with seawater or direct venting to the seafloor. These different subsurface processes are presented schematically in Figure 10 which shows a cross section through the Lucky Strike hydrothermal field with possible niches for microbial communities and different fluid flow paths. A typical spire complex growing through the silica rich hydrothermal slab records different fluid flow pathways or hydrothermal stages which affect the Se content, $\delta^{34}S$, $\delta^{82}Se$ and $\delta^{57}Fe$ of sulfides recovered at the seafloor (Fig. 10).

Stage (a). Direct venting of the end-member hydrothermal fluid. Sulfides deposited are Cu and Se-rich with $\delta^{82}Se$ and $\delta^{57}Fe$ close to basaltic values. The $\delta^{34}S$ value is typically around 1.5‰ reflecting the contribution of seawater sulfate in the reaction zone.

Stage (b). Cooling and mixing of the hydrothermal fluid with seawater penetrating at the base of the spire or in subsurface environment. The conductive cooling or seawater mixing form subsurface massive sulfide deposits. Chimney sulfides which are formed at lower temperatures are Cu- and Se-depleted and

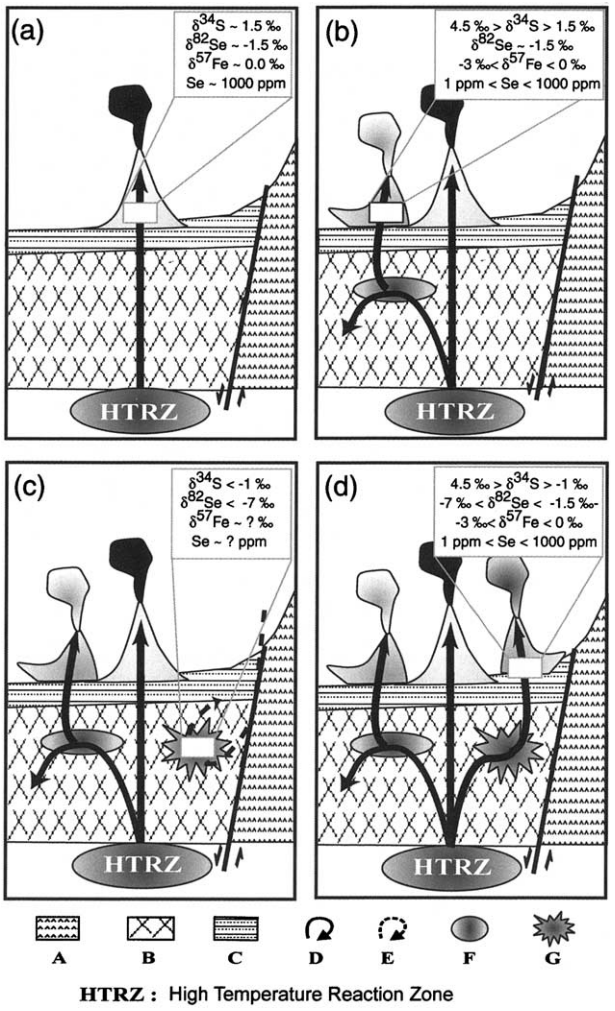

Fig. 10. Schematic representation of a cross section through the Lucky Strike hydrothermal field and different fluid flow paths. A: volcanic breccia of highly vesicular lava; B: altered substratum composed of tectonic breccia, related to the caldera faults, is the location for sulfide precipitation; C: silicified layered volcanic ejecta (Si/Ba slabs), relatively impermeable, where diffuse venting and disseminated sulfide precipitation occurs; D: high temperature metal-rich hydrothermal fluid convective cell; E: lower temperature metal-poor hydrothermal fluid diffuse circulation; F: (massive) sulfides precipitation at depth due to conductive cooling of the hydrothermal fluid and/or mixing of the hydrothermal fluid with seawater; G: low-temperature (<100°C) subsurface environment with high fluid flow representing a possible niche for microbial communities and reduction of S and Se (biotic or abiotic) oxyanions from seawater. A typical spire complex growing through the silica rich hydrothermal slab records different fluid flow pathways or hydrothermal stages which affect the Se content, $\delta^{34}S$, $\delta^{82}Se$ and $\delta^{57}Fe$ of sulfides recovered at the seafloor. Stage (a): Direct venting of the end-member hydrothermal fluid. Sulfides deposited are Cu and Se-rich with $\delta^{82}Se$ and $\delta^{57}Fe$ close to basaltic values. Stage (b): Mixing-cooling of the hydrothermal fluid with seawater penetrating at the base of the spire or in subsurface environment. Stage (c): Circulation of seawater through altered substratum with sulfate (anhydrite and barite) precipitation and reduction of Se oxyanion in suboxic warm environment. Stage (d): Remobilization and leaching of subsurface deposits formed during stage (c), producing variations in $\delta^{82}Se$ and $\delta^{34}S$ values in chimneys sulfides.

$\delta^{57}Fe$ is fractionated towards negative values as subsurface precipitation occurs. The $\delta^{82}Se$ values are not affected by this process whereas the $\delta^{34}S$ values may increase due to sulfate reduction.

Stage (c). Circulation of seawater through altered substratum with sulfate (anhydrite and barite) precipitation and reduction of Se oxyanions in suboxic warm environment. Se immobilization is likely to be mediated by Fe(II,III) hydrous oxides derived from altered massive sulfides at depth. Se isotopes are expected to be strongly fractionated towards negative values during this process. Microbial sulfate reduction may occur in this environment and produce H_2S with highly fractionated S isotopic composition.

Stage (d). Remobilization and leaching of subsurface deposits formed during stage (c), producing variations in $\delta^{82}Se$ and $\delta^{34}S$ values in chimneys sulfides.

7. CONCLUSIONS

Before this study, isotopic data for sulfur from MAR hydrothermal fields were reported from two drilled mounds at TAG (Chiba et al., 1998; Gemmell and Sharpe, 1998; Knott et al., 1998) and Snake Pit (Kase et al., 1990) and one active hydrothermal field at Broken Spur (Duckworth et al., 1995). Previous explanations of the low $\delta^{34}S$ of pyrite and/or marcasite were based on: (1) late-stage pyrite precipitation in the cores of chimneys at temperatures below 200°C with a low rate of sulfate reduction, or (2) lower fluid/rock interaction in the reaction zone, as well as more focused discharge in MAR hydrothermal systems which may produce low $\delta^{34}S$ in sulfide deposits, close to magmatic values. However, a careful examination of S isotope systematics in both low and high temperature vents, coupled with other geochemical tracers such as Se content and Se and Fe isotopes, suggests that low $\delta^{34}S$ data for pyrite (around 0‰) are more likely due to the effect of microbial sulfate reduction in warm subsurface environment. The use of S, Se and Fe isotope signatures of sulfide deposits also allows the identification of abiotic subsurface processes such as sulfide precipitation, seawater sulfate reduction by mixing with the high temperature hydrothermal fluid and Se oxyanion reduction and preconcentration.

Although abiotic fractionation of Se-isotopes can produce large variations, the effect of microbial respiration of selenium oxyanion cannot be excluded. The unexpectedly large $\delta^{82}Se$ variations in hydrothermal sulfides should provide some guidance for further studies of selenium biogeochemistry in seafloor hydrothermal systems. An important issue in this context is the capability for microbes to live in selenium-rich substrates and to find benefit from the use of selenium as electron acceptors.

An important implication of our finding is that light Fe isotope compositions down to 3.24‰ may be explained by equilibrium fractionation during sulfide precipitation in the subsurface environment, and thus be completely abiotic. Fe(III) acting as an electron acceptor has been reported in hot springs (Slobodkin et al., 2001). This has important implications for Fe mineralization (Bridge and Johnson, 1998) and may be associated with the evolution of microbial life (Vargas et al., 1998). However, our results provide further evidence for abiotic fractionation of Fe isotopes in hydrothermal systems. Thus, the variations in $\delta^{57}Fe$ towards negative values which are similar to those produced by Fe(III) bacterial reduction, require careful interpretation and an evaluation of the history of the fluids

before precipitation of sulfides. Furthermore, the present study highlights the need for an extensive experimental program for determining equilibrium isotope fractionation factors for sulfides and fluids in hydrothermal conditions.

Acknowledgments—We thank T. K. Kyser for the interlaboratory comparisons of sulfur isotope analyses. The technical expertise of M. Bohn for electron microprobe is gratefully acknowledged. This work benefited from useful reviews by J. Alt and an anonymous reviewer and comments by B. Beard. Technical support was provided by the PRISMS-EC grant, contract STM4CT 98-2220 and an IFREMER-CRPG jointly founded project.

Associate editor: S. Sheppard

REFERENCES

Alt J. C. (1988) The chemistry and sulfur isotope composition of massive sulfide and associated deposits on Green Seamount, Eastern Pacific. *Econ. Geol.* **83,** 1026–1033.

Anbar A. D., Roe J. E., Barling J., and Nealson K. H. (2000) Nonbiological fractionation of iron isotopes. *Science* **288,** 126–128.

Arnold M. and Sheppard S. M. F. (1981) East Pacific Rise at latitude 21°N: Isotopic composition and origin of the hydrothermal sulfur. *Earth Planet. Sci. Lett.* **56,** 148–156.

Auclair G., Fouquet Y., and Bohn M. (1987) Distribution of selenium in high-temperature hydrothermal sulfide deposits at 13°N, East Pacific Rise. *Can. Mineral* **25,** 577–587.

Bach W. and Humphris S. E. (1999) Relationship between the Sr and O isotope compositions of hydrothermal fluids and the spreading and magma-supply rates at ocean spreading centers. *Geology* **27,** 1067–1070.

Barton P. B. J. and Toulmin P. (1966) Phase relations in the Fe-Zn-S system. *Econ. Geol.* **61,** 815–849.

Beard B. L. and Johnson C. M. (1999) High precision iron isotope measurements of terrestrial and lunar materials. *Geochim. Cosmochim. Acta* **63,** 1653–1660.

Beard B. L., Johnson C. M., Cox L., sun H., Nealson K. H., and Aguilar C. (1999) Iron isotope biosignatures. *Science* **285,** 1889–1892.

Beard B. L., Johnson C. M., Skulan J. L., Nealson K. H., Cox L., and Sun H. (2003a) Application of. Fe isotopes to tracing the geochemical and biological cycling of Fe. *Chem. Geol.* **195,** 87–117.

Beard B. L., Johnson C. M., VonDamm K. L., and Poulson R. L. (2003b) Iron isotope constraints on Fe cycling and mass balance in oxygenated Earth oceans. *Geology* **31,** 629–632.

Belshaw N. S., Zhu X. K., Guo Y., and O'Nions R. K. (2000) High precision measurement of iron isotopes by plasma source mass spectrometry. *Int. J. Mass Spectrom.* **197,** 191–195.

Bethke P. M. and Barton P. B. (1971) Distribution of some minor elements between coexisting sulfide minerals. *Econ. Geol.* **66,** 140–163.

Bluth G. J. and Ohmoto H. (1988) Sulfide-sulfate chimneys on the East Pacific Rise, 11° and 13°N latitudes. Part II: Sulfur isotopes. *Can. Mineral* **26,** 505–515.

Boyd T. D. and Scott S. D. (2001) Microbial and hydrothermal aspects of ferric oxyhydroxides and ferrosic hydroxides: The example of Franklin Seamount, Western Woodlark Basin, Papua New Guinea. *Geochem. Trans.* **7,** doi:10.1039/b105277m.

Brantley S. L., Liermann L., and Bullen T. D. (2001) Fractionation of. Fe isotopes by soil microbes and organic acids. *Geology* **29,** 535–538.

Bridge T. A. and Johnson D. B. (1998) Reduction of soluble iron and reductive dissolution of ferric iron-containing minerals by moderately thermophilic iron-oxidizing bacteria. *Appl. Env. Microbiol.* **64,** 2181–2186.

Bullen T. D., White A. F., Childs C. W., Vivit D. V., and Schulz M. S. (2001) Demonstration of significant abiotic iron isotope fractionation in nature. *Geology* **29,** 699–702.

Canfield D. E. (2001) Isotope fractionation by natural populations of sulfate-reducing bacteria. *Geochim. Cosmochim. Acta* **65,** 1117–1124.

Charlou J. L., Donval J. P., Douville E., Jean-Baptiste P., Radford-Knoery J., Fouquet Y., Dapoigny A., and Stievenard M. (2000) Compared geochemical signatures and the evolution of Menez Gwen (37°50′N) and Lucky Strike (37°17′N) hydrothermal fluids, south of the Azores Triple Junction on the Mid-Atlantic Ridge. *Chem. Geol.* **171,** 49–75.

Chaussidon M., Albarède F. and Sheppard S. M. F. (1991) Ion probe δ^{34}S study of small scale variations in a hydrothermal chimney, East Pacific Rise at 21°N. In *Source, Transport and Deposition of Metals* (eds. M. Pagel and J. Leroy), pp. 609–614. Society for Geology Applied to Mineral Deposits.

Chiba H., Uchiyama N. and Teagle D. A. H. (1998) Stable isotope study of anhydrite and sulfide minerals at TAG hydrothermal mound, Mid-Atlantic Ridge, 26°N. In *Proceedings of the Ocean Drilling Program, Scientific Results*, Vol. 158 (eds. P. M. Herzig, S. E. Humphris, D. J. Miller and R. A. Zierenberg), pp. 85–90. Ocean Drilling Program.

Cooper M. J., Elderfield H., and Schultz A. (2000) Diffuse hydrothermal fluids from Lucky Strike hydrothermal vent field: Evidence for a shallow conductively heated system. *J. Geophys. Reas.* **105,** 19369–19375.

Coplen T. B. and Krouse H. R. (1998) Sulphur isotope data consistency improved. *Nature* **392,** 32.

Delaney J. R., Kelley D. S., Lilley M. D., Butterfield D. A., Baross J. A., Wilcock W. S., Embley R. W., and Summit M. (1998) The quantum event of oceanic crustal accretion: Impacts of diking at Mid-Ocean Ridges. *Science* **281,** 222–230.

Deming J. W. and Baross J. A. (1993) Deep-sea smokers: Windows to a subsurface biosphere? *Geochim. Cosmochim. Acta* **57,** 3219–3230.

Duckworth R. C., Knott R., Fallick A. E., Rickard D., Murton B. J. and Dover C. V. (1995) Mineralogy and sulphur isotope geochemistry of the Broken Spur sulfides, 29°N, Mid-Atlantic Ridge. In *Hydrothermal Vents and Processes*, Vol. 87 (eds. L. M. Parson, C. L. Walker and D. R. Dixon), pp. 175–189. Geological Society Special Publication.

Ellis A. S., Johnson T. M., Herbel M. J., and Bullen T. D. (2003) Stable isotope fractionation of selenium by natural microbial consortia. *Chem. Geol.* **195,** 119–129.

Fisk M. R., Giovannoni S. J., and Thorseth I. H. (1998) Alteration of oceanic volcanic glass: Textural evidence of microbial activity. *Science* **281,** 978–980.

Fouquet Y., Charlou J.-L., Costa I., Donval J.-P., Radford-Knoery J., Pelle H., Ondréas H., Lourenço N., Ségonsac M., and Kingston-Tivey M. (1994) A detailed study of the Lucky Strike hydrothermal site and discovery of a new hydrothermal site: Menez Gwen. Preliminary results of the DIVA1 cruise. *InterRidge News* **3,** 14–18.

Fouquet Y., Ondreas H., Charlou J. L., Donval J. P., Radford K. J., Costa I., Lourenco N., and Tivey M. K. (1995) Atlantic lava lakes and hot vents. *Nature* **377,** 201.

Fredrickson J. K. and Onstott T. C. (1996) Microbes deep inside the Earth. *Sci. Am.*(October), 68–73.

Gemmell J. B. and Sharpe R. (1998) Detailed sulfur-isotope investigation of the TAG hydrothermal mound and stockwork zone, 26°N, Mid-Atlantic Ridge. In *Proceedings of the Ocean Drilling Program, Scientific Results*, Vol. 158 (eds. P. M. Herzig, S. E. Humphris, D. J. Miller and R. A. Zierenberg), pp. 71–84. Ocean Drilling Program.

Govindaraju K. (1994) 1994 compilation of working values and sample description for 383 geostandards. *Geostand. Newsl.* **18,** 1–158.

Habicht K. S., Canfield D. E., and Rethmeier J. (1998) Sulfur isotope fractionation during bacterial reduction and disproportionation of thiosulfate and sulfite. *Geochim. Cosmochim. Acta* **62,** 2585–2595.

Herbel M. J., Johnson T. M., Oremland R. S., and Bullen T. D. (2000) Fractionation of selenium isotopes during bacterial respiratory reduction of selenium oxyanions. *Geochim. Cosmochim. Acta* **64,** 3701–3709.

Huston D. L., Sie S. H., Suter G. F., Cooke D. R., and Both R. A. (1995) Trace elements in sulfide minerals from Eastern Australian volcanic-hosted massive sulfide deposits: Part I. Proton microprobe analyses of pyrite, chalcopyrite, and sphalerite, and Part II. Selenium levels in pyrite: Comparison with δ^{34}S values and implications for source in volcanogenic hydrothermal systems. *Econ. Geol.* **90,** 1167–1196.

Janecky D. R. and Shanks W. C. (1988) Computational modeling of chemical and sulfur isotopic reaction processes in seafloor hydrothermal systems: Chimneys, massive sulfides, and subjacent alteration zones. *Can. Mineral* **26,** 805–825.

Jannasch H. W. (1995) Microbial interactions with hydrothermal fluids. In *Seafloor Hydrothermal Systems: Physical, Chemical, Biological and Geological Interactions,* Geophysical Monograph 91 (eds. S. E. Humphris, R. A. Zierenberg, L. S. Mullineaux and R. E. Thomson). American Geophysical Union, pp. 273–297.

Johnson T. M., Herbel M. J., Bullen T. D., and Zawislanski P. T. (1999) Selenium isotope ratios as indicators of selenium sources and oxyanion reduction. *Geochim. Cosmochim. Acta* **63,** 2775–2783.

Johnson C. M., Skulan J. L., Beard B. L., Sun H., Nealson K. H., and Braterman P. S. (2002) Isotopic fractionation between Fe(III) and Fe(II) in aqueous solutions. *Earth Planet. Sci. Lett.* **195,** 141–153.

Johnson C. M., Beard B. L., Beukes N. J., Klein C., and O'Leary J. M. (2003) Ancient geochemical cycling in the Earth as inferred from Fe isotope studies of banded iron formations from the Transvaal Craton. *Contrib. Mineral. Petrol.* **144,** 523–547.

Johnson T. M. and Bullen T. D. (2003) Selenium isotope fractionation during reduction by Fe(II)-Fe(III) hydroxide-sulfate (green rust). *Geochim. Cosmochim. Acta* **67,** 413–419.

Jorgensen B. B., Isaksen M. F., and Jannasch H. W. (1992) Bacterial sulfate reduction above 100°C in deep-sea hydrothermal vent sediments. *Science* **258,** 1756–1757.

Juniper S. K. and Fouquet Y. (1988) Filamentous iron-silica deposits from modern and ancient hydrothermal sites. *Can. Mineral* **26,** 859–869.

Kase K., Yamamoto M. and Shibata T. (1990) Copper-rich sulfide deposit near 23°N, Mid-Atlantic Ridge: Chemical composition, mineral chemistry and sulfur isotopes. In *Proceedings of the Ocean Drilling Program, Scientific Results,* Vol. 106/109 (eds. R. Detrick, J. Honnorez, W. B. Bryan and T. Juteau), pp. 163–173. Ocean Drilling Program.

Kerridge J. F., Haymon R. M., and Kastner M. (1983) Sulfur isotope systematics at the 21°N site, East Pacific Rise. *Earth Planet. Sci. Lett.* **66,** 91–100.

Knott R., Fallick A. E., Rickard D. and Bäcker H. (1995) Mineralogical and sulphur isotope characteristics of a massive sulphide boulder, Galapagos Rift, 85°55′W. In *Hydrothermal Vents and Processes,* Vol. 87 (eds. L. M. Parson, C. L. Walker and D. R. Dixon), pp. 207–222. Geological Society Special Publication.

Knott R., Fouquet Y., Honnorez J., Petersen S. and Bohn M. (1998) Petrology of hydrothermal mineralization: A vertical section through the TAG mound. In *Proceedings of the Ocean Drilling Program, Scientific Results,* Vol. 158 (eds. P. M. Herzig, S. E. Humphris, D. J. Miller and R. A. Zierenberg), pp. 5–26.

Krouse H. R. and Thode H. G. (1962) Thermodynamic properties and geochemistry of isotopic compounds of selenium. *Can. J. Chem.* **40,** 367–375.

Langmuir C., Humphris S., Fornari D., Van-Dover C., VonDamm K., Tivey M. K., Colodner D., Charlou J. L., Desonie D., Wilson C., Fouquet Y., Klinkhammer G., and Bougault H. (1997) Hydrothermal vents near a mantle hot spot; the Lucky Strike vent field at 37 degrees N on the Mid-Atlantic Ridge. *Earth Planet. Sci. Lett.* **148,** 69–91.

Leutwein F. (1972) Selenium. In *Handbook of Geochemistry,* Vol. II/3 (ed. K. H. Wedepohl), pp. 34-B-1–34-O-3. Springer.

L'Haridon S., Cilia V., Messner P., Raguénès G., Gambacorta A., Sleytr U. B., Prieur D., and Jeanthon C. (1998) *Desulfurobacterium thermolithotrophum* gen. nov., sp. nov., a novel autotrophic, sulphur-reducing bacterium isolated from a deep-sea hydrothermal vent. *Int. J. System. Bacteriol.* **48,** 701–711.

Machel H. G., Krouse H. R., and Sassen R. (1995) Products and distinguishing criteria of bacterial and thermochemical sulfate reduction. *Appl. Geochem.* **10,** 373–389.

Maréchal C. D., Télouk P., and Albarède F. (1999) Precise analysis of copper and zinc isotopic compositions by plasma-source mass spectrometry. *Chem. Geol.* **156,** 251–273.

Marin L., Lhomme J., and Carignan J. (2001) Determination of selenium concentration in sixty five reference materials for geochemical analysis by GFAAS after separation with thiol cotton. *Geostand. Newsl.* **25,** 317–324.

Matthews A., Zhu X. K., and O'Nions K. (2001) Kinetic iron stable isotope fractionation between iron (-II) and (-III) complexes in solution. *Earth Planet. Sci. Lett.* **192,** 81–92.

McCollom T. and Shock E. L. (1997) Geochemical constraints on chemolithoautotrophic metabolism by microorganisms in seafloor hydrotehrmal systems. *Geochim. Cosmochim. Acta* **61,** 4375–4391.

McKibben M. A. and Eldridge C. S. (1990) Radical sulfur isotope zonation of pyrite accompanying boiling and epithermal gold deposition: A SHRIMP study of the valles caldera, New Mexico. *Econ. Geol.* **85,** 1917–1925.

Myneni S. C. B., Tokunaga T. K., and Brown G. E., Jr.. (1997) Abiotic selenium redox transformations in the presence of Fe(II,III) oxides. *Science* **278,** 1106–1109.

Ohmoto H. and Goldhaber M. B. (1997) Sulfur and carbon isotopes. In *Geochemistry of Hydrothermal Ore Deposits,* 3rd ed. (ed. H. L. Barnes), pp. 517–611. Wiley.

Oremland R. S. (1994) Biogeochemical transformations of selenium in anoxic environments. In *Selenium in the Environment* (eds. W. T. Frankenberger and S. Benson), pp. 389–419. Marcel Dekker.

Parkes R. J., Cragg B. A., Bale S. J., Getliff J. M., Goodman K., Rochelle P. A., Fry J. C., Weightman A. J., and Harvey S. M. (1994) Deep bacterial biosphere in pacific ocean sediments. *Nature* **371,** 410–413.

Peter J. M. and Shanks W. C., III.. (1992) Sulfur, carbon, and oxygen isotope variations in submarine hydrothermal deposits of Guaymas Basin, Gulf of California, USA. *Geochim. Cosmochim. Acta* **56,** 2025–2040.

Polyakov V. B. and Mineev S. D. (2000) The use of Mössbauer spectroscopy in stable isotope geochemistry. *Geochim. Cosmochim. Acta* **64,** 849–865.

Rashid K. and Krouse H. R. (1985) Selenium isotopic fractionation during SeO_3^{2-} reduction to Se^0 and H_2Se. *Can. J. Chem.* **63,** 3195–3199.

Rees C. E. and Thode H. G. (1966) Selenium isotope effects in the reduction of sodium selenite and of sodium selenate. *Can. J. Chem.* **44,** 419–427.

Rouxel O., Ludden J. and Fouquet Y. (2001) Selenium and antimony isotope variations in natural systems determined by MC-ICP-MS: Experimental and field studies. *4th International Symposium on Applied Isotope Geochemistry,* Pacific Grove, California (abstr.)

Rouxel O., Ludden J., Carignan J., Marin L., and Fouquet Y. (2002) Natural variations of Se isotopic composition determined by hydride generation multiple collector coupled mass spectrometer. *Geochim. Cosmochim. Acta* **66,** 3191–3.

Rouxel O., Dobbek N., Ludden J. and Fouquet Y. (2003) Iron isotope fractionation during oceanic crust alteration (Site ODP 801). *Chem. Geol.* **202,** 155–182.

Schauble E. A., Rossman G. R., and Taylor H. P. (2001) Theoretical estimates of equilibrium Fe-isotope fractionations from vibrational spectroscopy. *Geochim. Cosmochim. Acta* **65,** 2487–2497.

Shanks W. C., Bischoff J. L., and Rosenbauer R. J. (1981) Seawater sulfate reduction and sulfur isotope fractionation in basaltic systems: Interaction of seawater with fayalite and magnetite at 200–350°C. *Geochim. Cosmochim. Acta* **45,** 1977–1995.

Shanks W. C. and Seyfried W. E. (1987) Stable isotope of vent fluids and chimney minerals, Southern Juan de Fuca Ridge: Sodium metasomatism and seawater sulfate reduction. *J. Geophys. Res.* **92,** 11387–11399.

Shanks W. C. (2001) Stable isotopes in seafloor hydrothermal systems. In *Stable Isotope Geochemistry,* Reviews in Minerology and Geochemistry Vol. 43 (eds. J.W. Valley and D. Cole), pp. 469–525. Minerological Society of America.

Sharma M., Polizzotto M., and Anbar A. D. (2001) Iron isotopes in hot springs along the Juan de Fuca Ridge. *Earth Planet. Sci. Lett.* **194,** 39–51.

Skirrow R. and Coleman M. L. (1982) Origin of sulphur and geothermometry of hydrothermal sulphides from the Galapagos Rift, 86°W. *Nature* **299,** 142–144.

Slobodkin A., Campbell B., Craig-Cary S., Bonch-Osmolovskaya E., and Jeanthon C. (2001) Evidence for the presence of thermophilic Fe(III)-reducing microorganisms in deep-sea hydrothermal vents at 13°N (East Pacific Rise). *FEMS Microbiol. Ecol.* **36,** 235–243.

Stetter K. O., Huber R., Blöchl E., Kurr M., Eden R. D., Fielder M., Cash H., and Vance I. (1993) Hyperthermophilic archaea are thriving in deep North Sea and Alaskan oil reservoirs. *Nature* **365,** 743–745.

Stevens T. O. and McKinley J. P. (1995) Lithoautotrophic microbial ecosystems in deep basalt aquifers. *Science* **270,** 450–454.

Stolz J. F. and Oremland R. S. (1999) Bacterial respiration of arsenic and selenium. *FEMS Microbiol. Rev.* **23,** 615–627.

Styrt M. M., Brackmann A. J., Holland H. D., Clark B. C., Pisutha-Arnond V., Eldridge C. S., and Ohmoto H. (1981) The mineralogy and the isotopic composition of sulfur in hydrothermal sulfide/sulfate deposits on the East Pacific Rise, 21°N latitude. *Earth Planet. Sci. Lett.* **53,** 382–390.

Summit M. and Baross J. A. (2001) A novel microbial habitat in the mid-ocean ridge subseafloor. *Proc. Natl. Acad. Sci. USA* **98,** 2158–2163.

Takai K., Komatsu T., Inagaki F., and Horikoshi K. (2001) Distribution of. Archaea in a black smoker chimney structure. *Appl. Environ. Microbiol.* **67,** 3618–3629.

Tischendorf G. and Ungethüm H. (1964) In the conditions of formation of clausthalite-galena and some observations on the distribution of selenium in galena as a function of oxidation potential and pH. *Geochem. Int.* **1,** 1205–1225.

VanderWalt T. N., Strelow F. W. E., and Verheij R. (1985) The influence of crosslinkage on the distribution coefficients and anion exchange behaviour of some elements in hydrochloric acid. *Solvent Extraction Ion Exchange* **3,** 723–740.

Vargas M., Kashefi K., Blunt-Harris E. L., and Lovley D. R. (1998) Microbiological evidence for Fe(III) reduction on early Earth. *Nature* **395,** 65–67.

VonDamm K. L., Edmond J. M., Grant B., Measures C. I., Walden B., and Weiss R. F. (1985) Chemistry of submarine hydrothermal solutions at 21°N, East Pacific Rise. *Geochim. Cosmochim. Acta* **49,** 2197–2220.

VonDamm K. L., Bray A. M., Buttermore L. G., and Oosting S. E. (1998) The geochemical controls on vent fluids from the Lucky Strike vent field, Mid-Atlantic Ridge. *Earth Planet. Sci. Lett.* **160,** 521–536.

Wirsen C. O., Jannasch H. W., and Molyneaux S. J. (1993) Chemosynthetic microbial activity at Mid-Atlantic ridge hydrothermal vent sites. *J. Geophys. Res.* **98,** 9693–9703.

Woodruff L. G. and Shanks W. C. (1988) Sulfur isotope study of chimney minerals and vent fluids From 21°N, East Pacific Rise: Hydrothermal sulfur sources and disequilibrium sulfate reduction. *J. Geophys. Res.* **93,** 4562–4572.

Yamamoto M. (1976) Relationship between Se/S and sulfur isotope ratios of hydrothermal sulfide minerals. *Min. Dep.* **11,** 197–209.

Yamamoto M., Kase K., and Ueda A. (1983) Fractionation of sulfur isotopes and selenium between coexisting pyrite and chalcopyrite from the Hitachi deposits, Ibaraki Prefecture, Japan. *Geochem. J.* **17,** 29–39.

Yamamoto M., Endo M., and Ujihira K. (1984) Distribution of selenium between galena and sphalerite. *Chem. Geol.* **42,** 243–248.

Zhu X. K., O'Nions R. K., Guo Y., Belshaw N. S., and Rickard D. (2000a) Determination of natural Cu-isotope variation by plasma-source mass spectrometry: Implications for use as geochemical tracers. *Chem. Geol.* **163,** 139–149.